Multiexciton complexes in semiconductors

V. D. Kulakovskiĭ, G. E. Pikus, and V. B. Timofeev

Institute of Solid State Physics, Academy of Sciences of the USSR, Chernogolovka, Moscow District and A. F. Ioffe Physicotechnical Institute, Academy of Sciences of the USSR, Leningrad
Usp. Fiz. Nauk **135**, 237–284 (October 1981)

The present state of research on multiexciton-impurity complexes is reviewed. These complexes are weakly bound nonequilibrium states of a shallow neutral impurity (a donor or acceptor) and several excitons in a semiconductor. Bound multiexciton complexes are stable because of the high degree of degeneracy of the bands of the semiconductor. The shell model for a multiexciton-impurity complex is discussed. According to this model, the electrons and holes in the complex fill shells successively in accordance with the Pauli principle. The shell model classifies the electron (or hole) states of the complex, with allowance for the local symmetry of the impurity center, and it predicts the number of lines in the spectra and their fine structure. The effects of the valley-orbit interaction and the crystal splitting on the fine structure in the spectrum are analyzed. The use of external agents (uniaxial deformations and magnetic fields) as tools for studying the internal structure of multiexciton-impurity complexes is discussed. Particular emphasis is placed on silicon, which has received the most experimental study.

PACS numbers: 71.55.Fr, 71.35. + z

CONTENTS

1. INTRODUCTION

In addition to the lines corresponding to the emission of free excitons, the emission spectra of semiconductors contain lines which result from the recombination of excitons bound by impurities. The possible existence of excitons bound to shallow impurities (exciton–impurity complexes) in semiconductors was first suggested by Lampert[1] back in 1958. Lampert studied an exciton bound to a neutral donor (ND) or neutral acceptor (NA) as an analog of a diatomic molecule. Bound states of an exciton with shallow impurities were discovered in a semiconductor (silicon) by Haynes[2] in 1960. Since then, excitons bound to charged centers and isoelectronic traps have been observed in addition to exciton–impurity complexes at neutral centers in many crystals.

In 1970 Kaminskiĭ and Pokrovskiĭ[3] observed a series of narrow lines, with energies below that of the emission line of an exciton–impurity complex at an acceptor, in the radiative-recombination spectra of boron-doped silicon at high excitation levels. Since longer-wavelength lines appear at high excitation levels,[3-5] these investigators interpreted the observed spectrum as resulting from the radiative recombination of a complex consisting of a neutral impurity center and several excitons bound by this center. We will denote by NDE_m

 0038-5670/81/100815-26$01.10

the state of a bound multiexciton complex containing a definite number (m) of bound excitons at a neutral donor, and by NAE_m the corresponding state at a neutral acceptor. Kaminskiĭ, Pokrovskiĭ, *et al.*[3-5] suggested that the longer-wavelength lines in the observed discrete spectrum corresponded to complexes having relatively large values of m. Studies by the Pokrovskiĭ group,[3-5] Sauer,[6] and Kosai and Gershenzon,[7] who observed new series of lines associated with other impurities in silicon and who made a detailed study of the dependence of the intensity of the lines of the series on the excitation level, confirmed Kaminskiĭ and Pokrovskiĭ's suggestion regarding the nature of these lines.[3] In contrast, the results of subsequent studies by Sauer and Weber[8,9] on the splitting in a magnetic field and in deformed silicon crystals of lines attributed to bound multiexciton complexes could not initially be explained by the model of multiexciton–impurity complexes, and Sauer and Weber[9] categorically rejected this model. Although their conclusion proved premature, their work itself[8,9] undoubtedly stimulated interest in the problem of multiexciton–impurity complexes. Experimental and theoretical work in recent years has not only confirmed the concept of multiexciton–impurity complexes but has also made much progress toward an understanding of their structure. There have been significant increases in the number of objects which have been studied and in the number of experimental methods which have been used.

Our purpose in this review is to outline the major results of experimental and theoretical research in this field. We will also point out several questions which require further study.

2. SHELL MODEL OF BOUND MULTIEXCITON COMPLEXES

The stability of bound multiexciton complexes containing several excitons in the indirect semiconductors Si, Ge, and SiC, among others, is a consequence of the high degree of band degeneracy. In a semiconductor with simple bands there can be only two electrons, with opposite spins, at the Γ point in a given 1s orbital state, but in silicon, which has extrema at the Δ points, there may be 12 electrons in this state, differing in either spin or Bloch function. In germanium the extrema of the conduction band are at the L points, and the degree of degeneracy of the electron ground state is eight. In all of these crystals the valence band is fourfold degenerate at the Γ extremum, so that four holes, with angular momenta $j_x = \pm 3/2, \pm 1/2$, may be in a given orbital state. The role played by the band degeneracy in stabilizing bound multiparticle states was illustrated some time ago by Wang and Kittel,[10] who used the particular model of a multi-valley semiconductor with an electron/hole effective-mass ratio $m_e/m_h \sim 0$ to demonstrate that such complexes could exist with a binding energy of the order of the exciton rydberg per bound pair. Even in the earliest papers on bound excitons,[11,12] the one-electron approximation was used for their description. In other words, it was assumed that the electrons and holes are in a self-consistent field whose symmetry is the same as that of the impurity center. The valley–orbit splitting of the ground state of the neutral donor was taken into account, and it was assumed that both of the electrons in the exciton–impurity complex at a neutral donor were in the lower of the Γ_1 split states, so that their spins were antiparallel. This model was successful in explaining the observed Zeeman splitting of the emission lines of exciton–impurity complexes in GaP and Si. A similar model was used by Dean *et al.*,[13] who studied the splitting of the emission lines of complexes in cubic SiC crystals in a magnetic field. They found that the identical number of Zeeman components for the lines of multiexciton–impurity complexes with different numbers of electron–hole pairs could be explained by assuming that the electrons and the holes in the complexes occupy one-particle states in accordance with the Pauli principle.

In a logical extension of these ideas, Kirczenow[14,15] suggested that in complexes at neutral donors (NDE_m) two electrons occupy the lower level of Γ_1, while the other $m-1$ electrons occupy upper levels which are split off as a result of the valley–orbit interaction. In silicon, for example, where the 12-fold degenerate ground state of a neutral donor is split into the three terms Γ_1, Γ_3, and Γ_5 by the interaction with the short-range field of the donor,[16] $m-1$ electrons occupy the Γ_3 and Γ_5 terms, which have essentially the same energy. The only exceptional case is lithium, for which the lower levels are Γ_3 and Γ_5. In germanium, the eightfold-degenerate ground state of a neutral donor is split into[16] Γ_1 and Γ_5, and the Γ_5 level is occupied in complexes with $m \geq 2$. The magnitude of the valley–orbit splitting, Δ_{VO}, like the binding energy, depends on the number of bound excitons and also on the particular impurity to which these excitons are bound. The ground state for a hole in an exciton–impurity complex in Si, Ge, and SiC is the fourfold-degenerate state Γ_8. For two holes, the ground states are correspondingly spin-antisymmetric states with total angular momenta $J = 0(\Gamma_1)$ and $J = 2$. The difference between the

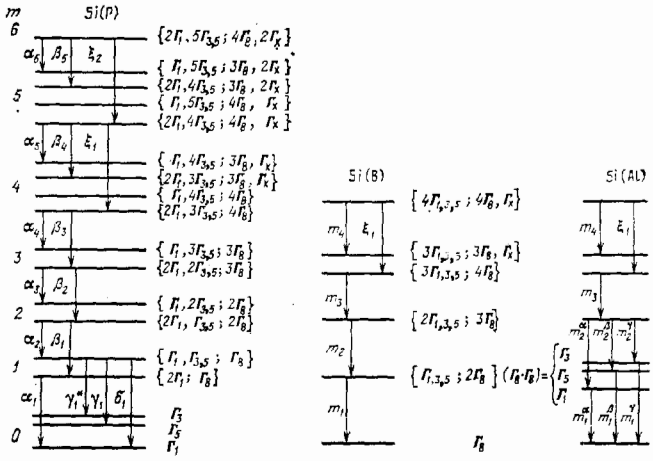

FIG. 1. Diagram of the optical transitions between the energy terms of multiexciton–impurity complexes at shallow neutral substitution impurities P, B, and Al in Si. P—Neutral donor; B and Al—neutral acceptors in the cases of weak and strong j–j interaction.

energies of these states is called the "j-j splitting." The $J=2$ state is split by the short-range potential of the impurity into the two terms[15] Γ_3 and Γ_5. The ground state for three holes is the Γ_8 state with $J=3/2$, while that for four holes is the non-degenerate Γ_1 state with $J=0$. The subsequent holes occupy excited states Γ_x which differ from the ground state by a smooth function. According to Lipair and Baldereschi,[17] the state nearest Γ_8 in silicon is the twofold-degenerate state Γ_7, to which a large contribution is made by the wave functions of the Γ_7 valence band, which is split off from the Γ_8 band by the spin–orbit interaction.

For excitons bound to neutral donors the j–j splitting, like the $\Gamma_3-\Gamma_5$ splitting, of the $J=2$ term is small and is ordinarily not reflected in the spectra. In this case it can be assumed that two holes occupy all states allowed by the Pauli principle, as shown in Fig. 1, which illustrates the occupation of the NDE_m states.[15] According to this scheme the NDE_m ground state in silicon can be described by

$$\left.\begin{array}{rl} \{2\Gamma_1;\ \Gamma_8\} & \text{for } m=1, \\ \{2\Gamma_1,\ (m-1)\,\Gamma_{3,5};\ m\Gamma_8\} & \text{for } 2\leqslant m\leqslant 4, \\ \{2\Gamma_1,\ (m-1)\,\Gamma_{3,5};\ 4\Gamma_8,\ (m-4)\,\Gamma_7\} & \text{for } m=5,6. \end{array}\right\} \quad (1)$$

According to the shell model, the lower-lying excited state of a multiexciton–impurity complex forms in the transition of one electron from the Γ_1 shell to $\Gamma_{3,5}$. For $m\leqslant 4$ these states are described by

$$\{\Gamma_1,\ m\Gamma_{3,5};\ \ m\Gamma_8\}. \quad (2)$$

The substantial decrease in the energy in the Γ_1 state for the neutral donor results from the large amplitude of the smooth wave function of the electron in the attractive potential of the central cell. In contrast, in complexes at neutral acceptors the electrons are repelled by the field of the ion from the central cell. Consequently, the splitting of the electronic states Γ_1 and $\Gamma_{3,5}$ is negligible for complexes bound by neutral acceptors in silicon, and there is essentially no evidence of this splitting in the spectra. In this case the lower-lying $\Gamma_{1,3,5}$ state may have up to 12 electrons. In an exciton–impurity complex at the shallowest acceptor, boron the j–j splitting is also small.[18,19] Figure 1 shows the scheme for the occupation of the states of a multiexciton–impurity complex at boron. According to this scheme, the NAE_m ground state in silicon can be described by

$$\begin{array}{ll} \{m\Gamma_{1,3,5};\ (m+1)\,\Gamma_8\} & \text{for } m\leqslant 3, \\ \{m\Gamma_{1,3,5};\ 4\Gamma_8,\ (m-3)\,\Gamma_7\} & \text{for } m=4,5. \end{array} \quad (3)$$

For complexes bound to deeper acceptors (Al, Ga, In) the luminescence spectra of NAE_m with one or two bound excitons clearly exhibit a line splitting caused[1)] by a splitting of the ground state of the holes in the complex into the three terms Γ_1, Γ_3, and Γ_5 (Refs. 15 and 20–22).

The degree of degeneracy of the terms in the shell model is higher than would follow from group theory for a cubic crystal, in which the maximum degree of degeneracy for states with integer spin is three, and that for states with half-integer spin is four. The reason for the difference is that the shell model ignores the correlations between particles, which should lead to a further splitting of terms. Parsons[26] has observed a fine structure in the emission lines of multiexciton–impurity complexes in silicon through the use of a high-resolution spectral apparatus (consisting of a grating monochromator and an interferometer). In germanium, where these splittings are larger, some additional fine structure of the levels of an exciton–impurity complex at a neutral donor has recently been discovered by Mayer and Lightowlers.[27] We turn now to a more detailed discussion of the reasons for the fine structure of the levels of multiexciton–impurity complexes.

3. EMISSION SPECTRA OF MULTIEXCITON–IMPURITY COMPLEXES IN SILICON

The recombination of electrons and holes in indirect semi-conductors is accompanied by a transfer of momentum to a phonon or an impurity. In silicon, transitions involving the emission (or absorption) of all four phonons—TO, TA, LO, and LA—are allowed. The corresponding emission lines are shifted from the no-phonon (NP) lines by the frequency of the corresponding phonon, with the wave vector $\mathbf{K}_\Delta$. In silicon the NP and TO lines are the most intense.

a) One-electron transitions

The most intense radiative transitions in complexes are the one-electron transitions, which give rise to a photon and to the formation of a new complex with a number of bound excitons smaller by one. As mentioned above, in complexes at substitution donors two electrons are in the Γ_1 lower level, while the other $m-1$ electrons are in an upper level, i.e., $\Gamma_{3,5}$ in silicon or Γ_5 in germanium. In this case, in complexes containing two or more excitons, transitions of two types are possible[15] (Fig. 1). First, there are the α transitions,

$$\{2\Gamma_1,\ (m-1)\,\Gamma_{3,5};\ m\Gamma_8\} \to \{\Gamma_1,\ (m-1)\,\Gamma_{3,5};\ (m-1)\,\Gamma_8\}, \quad (4)$$

in which the Γ_1 electron recombines, and the remaining complex is in an excited state. Second, there are the β transitions,

$$\{2\Gamma_1,\ (m-1)\,\Gamma_{3,5};\ m\Gamma_8\} \to \{2\Gamma_1,\ (m-2)\,\Gamma_{3,5};\ (m-1)\,\Gamma_8\}, \quad (5)$$

in which the $\Gamma_{3,5}$ electron recombines, and the system remains in the ground state. In an NDE_1 (two electrons of Γ_1), only the α transition is possible; the radiative decay leaves a neutral donor in the ground state. A crucial step toward an explanation for the spectra of multiexciton–impurity complexes at neutral donors was Kirczenow's suggestion[15] that all the lines observed in the no-phonon spectra of NDE_m in Si(P) (Fig. 2) were

[1)] In some early papers,[23,24] the splitting of the $J=2$ term was attributed to an exchange interaction of $J=2$ holes with an $s=1/2$ electron which led to the formation of two states with total angular momenta of 3/2 and 5/2. The observed splitting, however, was much larger than that expected for the silicon exchange splitting. Kirczenow[15] and Pikus[25] suggested that the appearance of three lines in the spectra might result from a splitting of the $J=2$ term by a short-range impurity field of symmetry T_d. For multiexciton–impurity complexes and neutral donors, as at boron centers, this splitting is slight because of the low density of the hole wave function at the center.

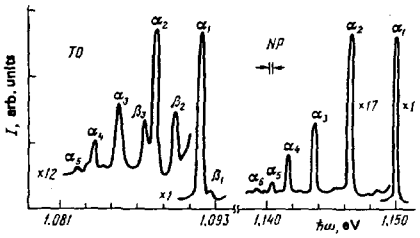

FIG. 2. Emission spectra of multiexciton–impurity complexes in Si(P) in the no-phonon (NP) region and also for the emission of TO phonons ($T = 4.2$ K; Ref. 18).

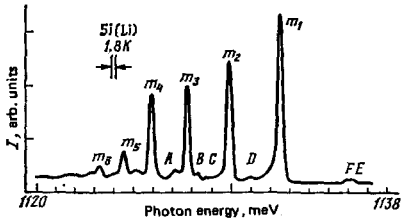

FIG. 3. Emission spectra of multiexciton–impurity complexes in Si(Li) involving the emission of a TA phonon ($T = 1.8$ K; Ref. 30).

consequences of the recombination of an electron from the Γ_1 state, i.e., that these were α lines. Although β lines are not forbidden in the NP spectra of silicon by the selection rules (more on this below), these lines are essentially not observed. The reason is that the combinations of Bloch functions corresponding to all the states of the $\Gamma_{3,5}$ term vanish at the center of the donor, where the short-range potential of the donor is at a maximum. The amplitude of the hole wave function at the donor is also small, so that the matrix element for the corresponding indirect NP transitions is small.

Emission lines resulting from the recombination of $\Gamma_{3,5}$ electrons have been observed by Thewalt[18] (Fig. 2) in the phonon components of the spectrum. In agreement with an increase in the fraction of $\Gamma_{3,5}$ electrons with increasing number of excitons in the complex, the intensity ratio of the β and α lines, $I(\beta_{m-1})/I(\alpha_m)$, increases with increasing m.

The binding energies of the excitons in the complexes, δ_m, can be determined from the positions of the α_1 line for $m = 1$ and the β_{m-1} line for $m = 2$–4. In Si(P), these energies are 4.58, 3.8, 6.69, and 9 meV for $m = 1$, 2, 3, and 4, respectively. The nonmonotonic behavior of δ_m at $m = 2$ occurs because a new electronic shell, $\Gamma_{3,5}$, begins to be filled in NDE_2. Lyon *et al.*[28] have attempted to determine the exciton binding energies in multiexciton–impurity complexes by a thermodynamic method. The values which they found for δ_1 and δ_2 are approximately equal to the values listed above, but their values of δ_3 and δ_4 are smaller by a factor of three or four. We do not rule out the possibility, however, that a thermodynamic equilibrium is not reached for short-lived multiexciton–impurity complexes with $m = 3$ and 4.

The difference between the frequencies of the β_m and α_{m-1} lines determines the magnitude of the valley–orbit splitting: $\Delta_{mVO} = \hbar\omega(\beta_{m-2}) - \hbar\omega(\alpha_{m-1})$. In Si(P), for multiexciton–impurity complexes with $m = 1$–3, the splitting Δ_{mVO} is about 4 meV (Ref. 18). As expected, this splitting is much smaller than the $\Gamma_1 - \Gamma_5$ splitting for a neutral donor (~12 meV). Furthermore, in contrast with the $\Gamma_1 - \Gamma_5$ splitting, the value of Δ_{mVO} in a neutral donor remains essentially constant from one donor to another.[24] We also note that $\Delta_{2VO} > \delta_2 = 3.8$ meV; in other words, an excited state of a multiexciton–impurity complex with two excitons in Si(P) is unstable with respect to the decay into an exciton–impurity complex and a free exciton. Nevertheless, it follows from the half-width of the α_3 emission line that the lifetime of this state is at least no shorter than 10^{-10} s.

In Si(Li) (a case of an interstitial donor), in which the electrons in multiexciton–impurity complex are in only the $\Gamma_{3,5}$ lower level at low temperatures, only a single line, m_m, correspond to each complex in the emission spectrum (Fig. 3). There is an analogous situation in a multiexciton–impurity complex at a neutral acceptor in the absence of j-j splitting [i.e., in Si(B) (Fig. 4)], since the Γ_1, Γ_3, and Γ_5 states have essentially the same energy for these centers, as mentioned earlier.

The exciton binding energies in multiexciton–impurity complexes in Si(Li) and Si(B) can be determined from the spectral positions of the m_m lines. The energy δ_m increases monotonically as the main electron and hole shells are filled (Table I). It can be seen from Table I that in Si(B) we have $\delta_3 \approx 2\delta_1$, while in Si(Li) we have $\delta_4 \approx 3\delta_1$.

In multiexciton–impurity complexes with $m \geq 5$ at neutral donors and in multiexciton–impurity complexes with $m \geq 4$ at neutral acceptors, the holes occupy the Γ_X upper shell in addition to the Γ_8 shell. In principle, therefore, it would be possible to observe in the emission spectra of such complexes two series of lines, resulting from the recombination of holes from the Γ_8 shell and from the Γ_X shell. Correspondingly, in the first case the multiexciton–impurity complex goes into an excited state:

$$\{m\Gamma_{1,3,5};\ 4\Gamma_8,\ (m-3)\,\Gamma_X\} \rightarrow \{(m-1)\,\Gamma_{1,3,5};\ 3\Gamma_8,\ (m-3)\,\Gamma_X\}. \quad (6)$$

During the recombination of a Γ_X hole, the multiexciton–impurity complex goes to the ground state:

$$\{m\Gamma_{1,3,5};\ 4\Gamma_8,\ (m-3)\,\Gamma_X\} \rightarrow \{(m-1)\,\Gamma_{1,3,5};\ 4\Gamma_8,\ (m-4)\,\Gamma_X\}. \quad (7)$$

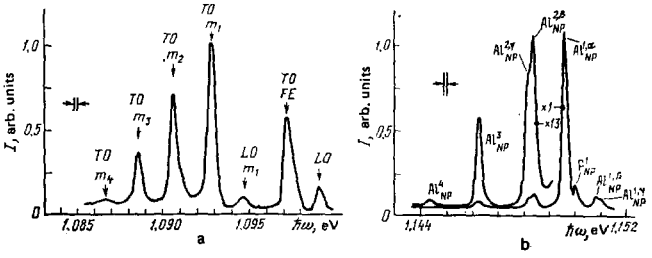

FIG. 4. Emission spectra of multiexciton–impurity complexes at acceptors. a—Si(B) (Ref. 19), $T = 1.8$ K; b—Si(Al) (Ref. 18), $T = 4.2$ K. The P^1_{NP} line results from the emission by an NDE_1 at a residual phosphorus impurity.

TABLE I. Binding energies of multiexciton–impurity complexes in silicon found by spectroscopic (δ) and thermodynamic (δ^*) methods (from the data of Refs. 18, 28, and 30).

	B		Al		P		Li
	δ[18]	δ^*[28]	δ[18]	δ^*[28]	δ[18]	δ^*[28]	δ[30]
1	3.9	3.6	5.1	4.4	4.6	4.9	3.4
2	6.1	6.0	5.2	4.6	3.8	5.8	5.9
3	8.3	6.1	8.5	6.8	6.7	4.5	8.15
4	—	3.0	—	—	—	3.3	10
5	—	—	—	—	—	2.2	7.5
6	—	—	—	—	—	—	8.8

Piezospectroscopic and magnetospectroscopic measurements (see Sections 6 and 7 below) have shown that the lines observed in the spectra of multiexciton– impurity complexes at neutral donors and neutral acceptors correspond to transitions of type (6), so that the binding energies δ_m cannot be determined from the positions of these lines in the case of complexes containing more than four holes. Transitions of the type in (7) for multiexciton–impurity complexes with $m = 5$ and 6 in Si(Li) may correspond to weak A and B lines[30] (Fig. 3), but these lines are faint, and so far they have received nothing approaching a detailed study. In Si(B) the emission line of a multiexciton–impurity complex corresponding to a transition of type (7) should lie on the violet side of m_4 in the vicinity of the intense lines $m_1 - m_3$, and it has not yet been distinguished from these intense lines.

In multiexciton–impurity complexes at neutral donors, the lines in (7) corresponding to the recombination of Γ_X holes with electrons from the Γ_1 inner shell should also be observed in the no-phonon spectrum, where the lines are narrower and much fewer in number (only α lines are present). The observation of these lines would make it possible to identify the Γ_X hole shell. As mentioned earlier, the j–j interaction of holes becomes important for acceptors deeper than boron in exciton–impurity complexes, and it leads to a splitting of the levels of the exciton–impurity complexes into the three terms Γ_1, Γ_3, and Γ_5. Figure 1 shows the transition scheme in this case; Fig. 5 shows the positions[18] of the corresponding lines for B, Al, and Ga.

In the emission spectra of excitons bound to neutral donors in silicon, lines in addition to the α and β lines appear when the temperature is raised to 19 K. These additional lines result from transitions from excited

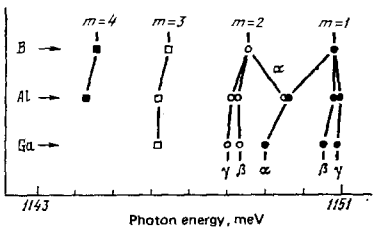

FIG. 5. Energy positions of the emission lines of multiexciton—impurity complexes in silicon doped with various acceptors.

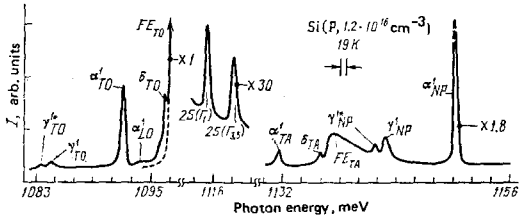

FIG. 6. Emission spectra of an NDE_1 in Si(P) ($T = 19$ K; Ref. 18).

states in which one of the electrons is excited from the Γ_1 level to the $\Gamma_{3,5}$ state[18] (Fig. 6). In this case there may be a recombination of the Γ_1 electron (the γ^1 and γ^{1*} transitions to an excited state of a neutral donor) and a $\Gamma_{3,5}$ electron (the δ transition to the ground state of the neutral donor). In Si(P), both of the lines, $\gamma^{(1)}$ and γ^{1*}, corresponding to transition to the Γ_5 and Γ_3 states of the neutral donor, are allowed; there is a slight difference in energy. Dean *et al.*[31] were apparently the first to observe transitions from an excited state of an exciton-impurity complex, but these transitions were not interpreted correctly on the basis of the shell model until the study by Thewalt,[18] who resolved all three of the lines γ^1, γ^{1*}, and δ in the Si(P) emission spectrum at 19 K. The δ transition had been observed slightly earlier in the modulation-absorption spectra[32] of Si(P), but it was interpreted incorrectly as a two-electron transition for a free exciton (see Ref. 33, for example).

b) Two-electron transitions in exciton–impurity complexes

In addition to the one-electron transitions which we have been discussing, the emission spectra of exciton–impurity complexes at phosphorus donors exhibit so-called two-electron transitions, in which one of the remaining electrons goes from the 1s ground state to the ns excited state. Specifically, these are the transitions[18,34]

$$\{2\Gamma_1\,(1s);\Gamma_8\} \to \{\Gamma_1\,(ns)\} \text{ с } n = 2 - 6 \tag{8}$$

and the transitions[18] (Fig. 6)

$$\{\Gamma_1,\ \Gamma_{3,5}\,(1s);\ \Gamma_8\} \to \{\Gamma_{3,5}\,(2s)\}. \tag{9}$$

The emission lines corresponding to these transitions are much less intense than the α_1 or δ lines. Strictly speaking, transitions (8) and (9) are not allowed by the one-electron model, since the wave functions of the 1s electrons in an exciton–impurity complex are not orthogonal with respect to the wave functions of the ns electrons at a neutral donor. From this standpoint, the difference between transitions (8), (9) and (4), (5) is quantitative, and Kirczenow[15] suggests that these transitions also be referred to as one-electron transitions.

The shell model also forbids transitions in which the final electron state is orthogonal with respect to the initial state. For example, the transitions[15]

$$\{2\Gamma_1\,(1s);\ \ \Gamma_8\} \to \Gamma_{3,5}\,(ns) \tag{10}$$

with $n = 1, 2, \ldots$, are forbidden, since any state Γ_1 is orthogonal with respect to any state $\Gamma_{3,5}$. Transitions

of this type have not been observed in weakly doped silicon crystals, in either the no-phonon spectra or the spectra of the corresponding phonon repetitions.

In general, i.e., when correlations between the particles in the complex are taken into account, it is necessary to deal with the overall representations of the initial and final states, rather than the representations of the individual particles. When this general approach is taken, group theory does not, for example, forbid transitions of type (10) (Ref. 15). Such transitions have in fact been observed in germanium, where the correlation splittings are much larger than in silicon (Section 4).

4. FINE STRUCTURE OF THE LEVELS OF EXCITON–IMPURITY COMPLEXES IN GERMANIUM

In germanium, in contrast with silicon, the existence of multiexciton–impurity complexes has been firmly established only for complexes with one or two bound excitons.[27,35]

Mayer and Lightowlers[27] have observed a fine structure of the levels of an exciton bound to a neutral donor (Bi, P, As). This fine structure has been found in both the no-phonon luminescence spectra associated with the $NDE_2 - NDE_1$ and $NDE_1 - ND$ transitions and in the absorption spectra associated with the excitation of a bound exciton and an LA phonon.

Figure 7 shows the fine structure of the lines of exciton–impurity complexes bound to As and P.

In germanium, the fourfold-degenerate state of the neutral donor is split into the two terms Γ_1 and Γ_5 by the valley–orbit interaction. According to the shell model, the electrons in the ground state of the exciton–impurity complex occupy both Γ_1 spin states, while in the first excited state they occupy one Γ_1 state and one Γ_5 state. The spectra in Fig. 7 correspond to transitions to the ground and first excited states of the neutral donor. As mentioned above, the shell model ignores electron–electron and electron–hole correlations. Group theory predicts that the $\{\Gamma_1, \Gamma_5; \Gamma_8\}$ excited state should split in two as a result of electron–electron correlations; the two resulting states would correspond to the products $(\Gamma_1 \cdot \Gamma_5)$ which are symmetrized and antisymmetrized with respect to the orbital states. The wave function of the $\{(\Gamma_1 \cdot \Gamma_5)_s; \Gamma_8\}$ state, which contains the symmetrized product of the wave functions of different valleys, is antisymmetrized in terms of spin (the total spin of the two 1s electrons is zero). States with $S = 1$ and $S_z = \pm 1, 0$, which are symmetrized in terms of the spin, correspond to the $\{(\Gamma_1 \cdot \Gamma_5)_{as}; \Gamma_8\}$ terms which are antisymmetrized with respect to orbital states. The $\{2\Gamma_5; \Gamma_8\}$ upper excited state splits into four terms, which correspond to $(\Gamma_5 \cdot \Gamma_5)_s = \Gamma_{1s} + \Gamma_{3s} + \Gamma_{5s}$ and $(\Gamma_5 \cdot \Gamma_5)_{as} = \Gamma_{5as}$.

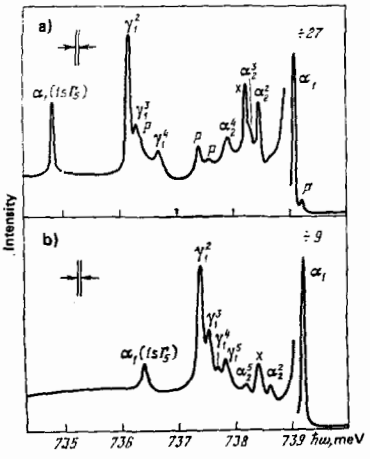

FIG. 7. Emission spectra of multiexciton–impurity complexes at a donor in germanium in the no-phonon region ($T = 1.5$ K; Ref. 27). The subscript gives the number of excitons bound in the complex. a—Ge(As); b—Ge(P).

The Γ_{1s} state may mix with the Γ_1 ground state, and the Γ_{5s} and Γ_{5as} states may mix with the corresponding terms of the first excited level, with resulting changes in their energies and wave functions. The reason for the splitting of the symmetrized and antisymmetrized states is a difference between the energies of the two electrons in the same or different valleys. Because of the pronounced anisotropy of the effective masses in germanium ($m_{e\parallel} \approx 20 m_{e\perp}$), the wave function of an electron at a donor in each valley is contracted along the principal axis of the valley. Because of the slighter overlap of wave functions, the energy of the Coulomb repulsion is less for electrons in different valleys than for electrons in the same valley. A similar splitting of one- and two-valley states has been observed[37,38] at D^- centers in germanium and silicon. We will call this effect "correlation splitting." If the magnitude of the valley–orbit splitting is Δ_{1VO}, and the difference between the energies of the one- and two-valley states of two electrons is Δ_{cor}, the energy of the $\{2\Gamma_1; \Gamma_8\}$ ground state is[36]

$$E(\Gamma_1) = \Delta_{1VO} + \frac{1}{2}\Delta_{cor} - \sqrt{\Delta_{1VO}^2 + \frac{1}{2}\Delta_{1VO}\Delta_{cor} + \frac{1}{4}\Delta_{cor}^2}, \quad (11)$$

and the energy of the two $\{\Gamma_1, \Gamma_5; \Gamma_8\}$ split terms is

$$E(\Gamma_{5s}) = \frac{3}{2}\Delta_{1VO} + \frac{1}{2}\Delta_{cor} - \frac{1}{2}\sqrt{\Delta_{1VO}^2 + \Delta_{cor}^2}, \quad (12)$$

$$E(\Gamma_{5as}) = \Delta_{1VO}. \quad (13)$$

for the $\{2\Gamma_5; \Gamma_8\}$ excited states,

$$E(\Gamma_{3s}) = E(\Gamma_{4s}) = 2\Delta_{1VO}, \quad (14)$$

$$E(\Gamma_{5s}) = \frac{3}{2}\Delta_{1VO} + \frac{1}{2}\Delta_{cor} + \frac{1}{2}\sqrt{\Delta_{1VO}^2 + \Delta_{cor}^2}, \quad (15)$$

$$E(\Gamma_{1s}) = \Delta_{1VO} + \frac{1}{2}\Delta_{cor} + \sqrt{\Delta_{1VO}^2 + \frac{1}{2}\Delta_{1VO}\Delta_{cor} + \frac{1}{4}\Delta_{cor}^2}. \quad (16)$$

Under the condition $\Delta_{cor} \ll \Delta_{1VO}$, the splitting of the $\{\Gamma_1, \Gamma_5; \Gamma_8\}$ term is thus $\Delta_{1VO}/2$. The correlation between electrons and holes should lead to a further splitting of the degenerate states. In principle there are two mechanisms for electron–hole interactions which would lift the degeneracy. One is electron–hole exchange, which leads to a splitting of the terms with a hole angular momentum of 3/2 and an electron angular momentum of $S = 1$ into three levels with total angular momenta of 1/2, 3/2, and 5/2. Estimates put the exchange splitting in germanium no higher than 0.1 meV, and it has not been observed experimentally. The second mechanism involves the crystal splitting of the Γ_8 hole ground state in the exciton into the two terms

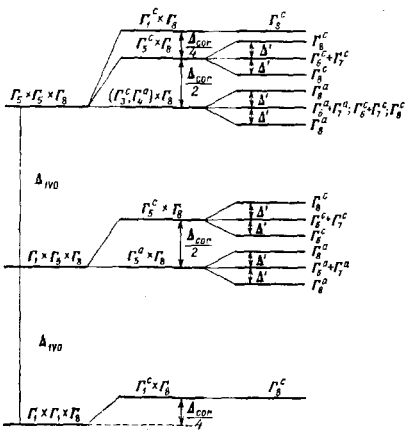

FIG. 8. Splitting of the NDE_1 levels in germanium.[36] $\Delta' = (1/4)\Delta_{cr}$; Δ_{cor} is the correlation splitting.

$L_4 + L_5$ and L_6. This splitting is caused by the nonspherical electron distribution, which is a consequence of the anisotropy of the effective mass. The $L_4 + L_5$ and L_6 states correspond to projections of hole angular momenta of $\pm 3/2$ and $\pm 1/2$ onto the direction of the given extremum. The crystal splitting Δ_{cr} for a free exciton in germanium is[39,40] about 1 meV, while that in silicon is[41] about 0.3 meV. In an exciton–impurity complex, the crystal splitting splits the $\{\Gamma_5; \Gamma_8\}$ term into three parts, Γ_8, Γ_8 and $(\Gamma_6 + \Gamma_7)$; the $\{\Gamma_3; \Gamma_8\}$ state splits in two, Γ_8 and $(\Gamma_6 + \Gamma_7)$. The energies calculated for the Γ_6 and Γ_7 states are identical. The crystal splitting also mixes the Γ_{8s}, Γ_{8as}, or $(\Gamma_6 + \Gamma_7)_s$ states, which derive from different terms. Figure 8 shows the level scheme of the exciton–impurity complex which results from correlation and crystal splittings.[36] Also shown here are the level shifts calculated under the conditions $\Delta_{cor} \ll \Delta_{1VO}$ and $\Delta_{cr} \ll \Delta_{1VO}$. For the $\{2\Gamma_5; \Gamma_8\}$ states, it also assumed that $\Delta_{cr} \ll \Delta_{cor}$. In this approximation, the energy of the three states $\Gamma_6 + \Gamma_7$, Γ_8, and $\Gamma_6 + \Gamma_7$ does not change. If only the crystal splitting is taken into account (with $\Delta_{cor} = 0$), we find a complete splitting of the terms in accordance with Fig. 7. According to this scheme, the $\{\Gamma_1, \Gamma_5; \Gamma_8\}$ state should split into six sublevels. Mayer and Lightowlers[27] have observed four levels for arsenic and five for phosphorus. Further experiments will be required to identify these levels and to determine the correlation and crystal splittings. In particular, it would be worthwhile to study the behavior of these levels in a magnetic field and upon deformation. For an exciton bound to a neutral acceptor, the valley–orbit splitting is apparently always small. As mentioned above, when the cubic anisotropy of the acceptor field is taken into account, the exchange interaction splits the two-hole state $(\Gamma_8 \cdot \Gamma_8)_{as}$ into the three terms Γ_1, Γ_5, and Γ_3. We denote the $\Gamma_5 - \Gamma_1$ splitting by Δ_{ex}, and we denote the splitting $\Gamma_3 - \Gamma_1$ by Δ'_{ex}. The Coulomb interaction of the holes with the electron in a definite valley lowers the symmetry from T_d to C_{3v}. As a result, the Γ_5 state splits into L_1 and L_3, and the Γ_1 and Γ_3 states transform into L_1 and L_3, respectively. There may be a mixing of the L_1 states which derive from Γ_1 and Γ_5 and also of the L_3 terms which derive from Γ_3 and Γ_5 (Fig. 8). When the crystal splitting is taken account, the energy of states 1 and 4 corresponding to the Γ_1 representations is

$$E_{1,4} = \frac{1}{2}\Delta_{ex} \pm \sqrt{\frac{1}{2}\Delta_{ex}^2 + \Delta_{cr}^2}. \tag{17}$$

The energies of the other levels do not change; i.e.,

$$E_{2,3} = \Delta_{ex} \text{ and } E_{5,6} = \Delta'_{ex}. \tag{18}$$

Each of these levels is fourfold degenerate in the number of valleys and twofold in the electron spin.

The magnitude of the crystal splitting for one hole, Δ_{cr}, in (17) may differ from the value of Δ_{cr} for a free exciton and for an exciton bound to a neutral donor. According to (18), there is no mixing of the L_3 states which derive from Γ_3 and Γ_5. This result is a consequence of the approximations made in the derivation of (17) and (18): In accordance with the shell model, it was assumed that the wave function of the two holes is an antisymmetrized product of the wave functions of each of the holes or the sum of such products, transformed according to the corresponding representation.

5. SELECTION RULES FOR TRANSITIONS IN MULTIEXCITON–IMPURITY COMPLEXES IN SILICON AND GERMANIUM

In the one-electron approximation, which is the basis of the shell model, the selection rules for transitions from a state of a multiexciton–impurity complex with m excitons to a state with $m-1$ or $m+1$ excitons are determined by the selection rules for the recombination or production of an individual electron–hole pair. For indirect transitions, the emission or absorption of a photon can occur only upon the simultaneous emission (or absorption) of a phonon or upon the transfer of momentum to an impurity center. Indirect transitions in silicon may be thought of as resulting from the virtual transfer of a Γ_{25} hole to one of the Δ bands or the virtual transition of a Δ_1 electron to one of the Γ bands, followed by a direct recombination (or by the direct excitation of a pair, in turn followed by the scattering of the electron or hole). Indirect transitions in germanium are accompanied by the scattering of an L_1 electron into one of the Γ bands or of a Γ_{25} hole into one of the L bands. The interference of all possible channels must be taken into account in calculating the transition probability.

The use of a method of invariants based on general symmetry considerations makes it possible to determine the general form of the transition matrix elements without considering the specific contribution of each channel. These selection rules are determined exclusively by the group symmetry of the wave vector at the extrema and by the representations under which the electron and hole wave functions transform at the extremum.

Table II shows the selection rules for Δ_6 electrons and Γ_8 holes in silicon and for L_6 electrons and Δ_8 holes in germanium found by this method.[25,42] These rules hold for both pairs of free carriers and free excitons. In Table II, the z axis is directed along the principal axis of the corresponding extremum; for germanium,

TABLE II. Selection rules for indirect transitions in germanium and silicon.

a) Ge, $\Gamma_8^+ - L_6$

j_z, s_z	3/2, −1/2	−3/2, 1/2	1/2, 1/2	−1/2, −1/2	1/2, −1/2	−1/2, 1/2
Phonon						
LA	$-\eta e_- u_{LA}$	$\eta e_+ u_{LA}$	$\frac{1}{\sqrt{3}}\eta e_- u_{LA}$	$-\frac{1}{\sqrt{3}}\eta e_+ u_{LA}$	$\sqrt{\frac{2}{3}}\lambda e_z u_{LA}$	$-\sqrt{\frac{2}{3}}\lambda e_z u_{LA}$
TO	$-(\alpha e_z u_- + \gamma e_+ u_+)$	$\alpha e_z u_+ - \gamma e_- u_-$	$\frac{1}{\sqrt{3}}(\alpha e_z u_- + \gamma e_+ u_+)$	$-\frac{1}{\sqrt{3}}(\alpha e_z u_+ + \gamma e_- u_-)$	$-\sqrt{\frac{2}{3}}\beta(e_+ u_- + e_- u_+)$	$\sqrt{\frac{2}{3}}\beta(e_+ u_- + e_- u_+)$
NP	$-\bar{\eta} e_-$	$\bar{\eta} e_+$	$\frac{1}{\sqrt{3}}\bar{\eta} e_-$	$-\frac{1}{\sqrt{3}}\bar{\eta} e_+$	$\sqrt{\frac{2}{3}}\bar{\alpha} e_z$	$-\sqrt{\frac{2}{3}}\bar{\lambda} e_z$

b) Si, $\Gamma_8^+ - \Delta_6$

j_z, s_z	3/2, −1/2	−3/2, 1/2	1/2, 1/2	−1/2, −1/2	1/2, −1/2	−1/2, 1/2
Phonon						
LA	$-\gamma e_+ u_{LA}$	$-\gamma e_- u_{LA}$	$\frac{1}{\sqrt{3}}\gamma e_+ u_{LA}$	$\frac{1}{\sqrt{3}}\gamma e_- u_{LA}$	0	0
LO	$-\eta e_- u_{LO}$	$\eta e_+ u_{LO}$	$\frac{1}{\sqrt{3}}\eta e_- u_{LO}$	$-\frac{1}{\sqrt{3}}\eta e_+ u_{LO}$	$\sqrt{\frac{2}{3}}\lambda e_z u_{LO}$	$-\sqrt{\frac{2}{3}}\lambda e_z u_{LO}$
TO, TA	$-\alpha e_z u_-$	$\alpha e_z u_+$	$\frac{1}{\sqrt{3}}\alpha e_z u_-$	$-\frac{1}{\sqrt{3}}\alpha e_z u_+$	$-\sqrt{\frac{2}{3}}\beta(e_+ u_- + e_- u_+)$	$\sqrt{\frac{2}{3}}\beta(e_+ u_- + e_- u_+)$
NP	$-(\bar{\gamma} e_+ + \bar{\eta} e_-)$	$-(\bar{\gamma} e_- - \bar{\eta} e_+)$	$\frac{1}{\sqrt{3}}(\bar{\gamma} e_+ + \bar{\eta} e_-)$	$\frac{1}{\sqrt{3}}(\bar{\gamma} e_- - \eta e_+)$	$\sqrt{\frac{2}{3}}\bar{\alpha} e_z$	$\sqrt{\frac{2}{3}}\bar{\lambda} e_z$

the x axis is chosen to lie in one of the σ_v planes, while in silicon the directions of the x and y axes are left arbitrary. Here j_z and s_z are the projections of the hole angular momentum ($j_z = \pm 3/2, \pm 1/2$) and the electron spin ($s_z = \pm 1/2$). In silicon, indirect transitions involving all phonons are allowed: the longitudinal acoustic (LA) phonon, with the displacement amplitude u_{LA}, which corresponds to the Δ_1 representation; the longitudinal optical (LO) phonon (u_{LO}; the Δ_2' representation); and the transverse TO and TA phonons (the Δ_5 representation). (In Table II it is assumed that the corresponding displacements u_x and u_y transform as yz and xz.) We see that the selection rules in scattering by LA phonons are determined by the single constant γ, while those for scattering by LO, TO, and TA phonons are determined by two constants: λ and η or α and β.

To determine the selection rules for a no-phonon line it is convenient to write the impurity potential $V(r)$, which does the scattering and which transforms under the Γ_1 representation of the group T_d, as the sum of potentials $V^+(r)$ and $V^-(r)$ which are even and odd with respect to the operation C_{4v}, which appears in the group $\Delta(C_{4v})$ but not in the group T_d. The potentials V^+ and V^- transform under the representations Δ_1 and Δ_2' of the Δ group. Knowing these representations, we can determine the selection rules given in Table II. The constant $\bar{\gamma}$ is related to scattering by V^+, while $\bar{\lambda}$ and $\bar{\eta}$ are related to scattering by V^-. In silicon, transitions through different bands make comparable contributions. For transitions exclusively through the band Γ_5, the constants $\alpha = \beta$, γ, and $\bar{\gamma}$ are nonzero. For transitions through Δ_5, the constants β, γ, η, $\bar{\gamma}$, and $\bar{\eta}$ are nonzero. For transitions through Γ_2', we have $\eta = \lambda$ and $\bar{\eta} = \bar{\lambda}$; the other constants are zero. In germanium, indirect transitions from the point L in Γ are allowed only if they involve an LA phonon with an amplitude u_{LA} (the L_2 representation) and TO phonons with amplitudes u_x and u_y (the L_3 representation). The selection rules for an LA phonon are determined by the two constants λ and η, while those for a TO phonon are determined by the three constants α, β, and γ (Ref. 42). A transition involving LO and TA phonons is allowed away from the extrema.[43] In the determination of the selection rules for no-phonon transitions, the impurity potential $V(r)$ is written as the sum of potentials V^+ and V^- which are even and odd with respect to the inversion i, which is included in the group $L(C_{3v} \cdot i)$ but not in T_d. The potentials V^+ and V^- transform under representations L_1 and L_2' of group L. Transitions from point L in Γ are allowed only if accompanied by scattering by the potential V^-, and the selection rules are determined by the two constants $\bar{\lambda}$ and $\bar{\eta}$.

In germanium, the energy distance between the extrema Γ_2' and L_1 is much smaller than the distance from L_1 or Γ_{25}' to any other extremum. The basic contribution to the LA and NP lines therefore comes from transitions through the Γ_2' band. When only these transitions are taken into account, we have $\eta = \lambda$, $\bar{\eta} = \bar{\lambda}$, and the selection rules for the LA and NP lines are the same as those for direct $\Gamma_2' - \Gamma_{25}'$ transitions. Transitions through the L_3' band contribute to only η and $\bar{\eta}$, and transitions through the L_2' band contribute to only λ and $\bar{\lambda}$. For transitions through the Γ_{15} band we have $\lambda = -2\eta$, $\bar{\lambda} = -2\bar{\eta}$. Transitions involving TO phonons through the band Γ_2 are forbidden. Transitions through the L_3' band contribute only to γ; those through L_2' contribute only to α; and those through Γ_{15} only to $\alpha = \beta = \gamma/2$.

Table II does not allow for the possible mixing of states from other bands with the L_6 and Γ_8^+ terms which derive from L_1 and Γ_{25}'. This mixing would result from the spin–orbit interaction. In this approximation, optical transitions from the (3/2, 1/2) and (−3/2; −1/2) states are forbidden. The possible mixing of other excited states with the terms with $j_z = \pm 3/2$ and $j_z = \pm 1/2$ which results from the crystal splitting is not taken into account for the indirect excitons. If the splitting is comparable to the binding energy, the oscillator strengths for transitions to these states may be slightly different, but the dependence of the matrix elements on

TABLE III. Relative intensities of the emission lines during the recombination of Γ_i electrons, averaged over all the possible hole states in germanium and silicon.

Term	Si	Ge
Γ_1	$(2\bar{\eta}+\bar{\alpha})^2$	$(2\bar{\eta}+\bar{\alpha})^2$
Γ_3	$2(\bar{\eta}-\bar{\alpha})^2$	—
Γ_5	$6\bar{\gamma}^2$	$2(\bar{\eta}-\bar{\alpha})^2$

the direction of the polarization vector e will not change.

Using Table II, and knowing the wave functions of the electrons and holes in the multiexciton–impurity complexes, we can find the selection rules for transitions involving the recombination of a definite pair in the complex.[2)] For phonon transitions, the probabilities for transitions through different extrema, corresponding to the emission of phonons with the corresponding wave vector **K**, are additive. The selection rules for the electron states Γ_1, Γ_3, and Γ_5 in silicon or Γ_1 and Γ_5 in germanium are therefore identical, and the intensities of these lines (with equal populations) are proportional to the statistical weights of these states. For the no-phonon lines, in contrast, it is the transition matrix elements which are additive, so that the transition probabilities for different electron states are different. The selection rules for the Γ_1 states in silicon and germanium are the same as the selection rules for the direct exciton $\Gamma_8^+ \cdot \Gamma_2'$. Table III shows the relative intensities of the lines associated with the recombination of Γ_1, Γ_3, and Γ_5 electrons in silicon and Γ_1 and Γ_5 electrons in germanium, averaged over all possible states of the holes and summed over the degenerate states of the electrons (i.e., the degeneracy of the Γ_3 and Γ_5 terms is taken into account). As mentioned in Section 3, the β lines associated with the recombination of $\Gamma_{3,5}$ electrons are essentially not observed in the no-phonon spectra of silicon. The constants $\bar{\gamma}$ and $(\bar{\eta} - \bar{\alpha})$ are therefore small.[3)] The reason is that for the Γ_3 and Γ_5 states the value of the corresponding combinations of Bloch functions vanishes at the point at which the potential $V(r)$ reaches its maximum.

The transition probabilities for the two-hole states Γ_1, Γ_3, and Γ_5 which are formed as a result of spin–orbit splitting are identical, so that the intensities of these lines, for equal populations, are proportional to the statistical weights of the states, 1 : 2 : 3.

In the sections which follow we will use these selection rules to calculate the polarization of the emission in a magnetic field and in a deformed crystal.

[2)] The selection rules for the phonon lines of excitons bound at a center may differ slightly from the selection rules for free excitons, because the transition matrix element M for the free excitons is proportional to $f(r)|_{r=r_e-r_h=0}$, while that for the bound excitons is given by $M \sim \int f_e(r) f_h(r)\, d^3r$. Consequently, the intensity of the transitions for states with $j_z = \pm 3/2$ and $j_z = \pm 1/2$ may be slightly different in the absence of crystal splitting. This circumstance can be taken into account by introducing additional factors $(1+\varkappa)$ and $(1-\varkappa)$ in the matrix elements of the transitions to these states. For the no-phonon transitions which are accompanied by the transfer of a large momentum $K \sim 1/a$ to the impurity (a is the lattice constant) the transition matrix element is determined by the short-range component of the impurity potential $V(r)$ at $r \sim a$. For such transitions we thus have $M \sim f_e(0) f_h(0)$, and the corresponding selection rules are the same as those for free excitons.

[3)] Kirczenow[14] has pointed out that the degree of polarization observed for the no-phonon emission line of free carriers in Si(B) in a longitudinal magnetic field agrees best with the theoretical results under the condition $[(\bar{\alpha} - \bar{\eta}) + 3\bar{\gamma}^2]/(2\bar{\eta} + \bar{\alpha})^2 = 0.18$.

6. EFFECT OF UNIAXIAL ELASTIC DEFORMATION ON THE EMISSION SPECTRA OF MULTIEXCITON–IMPURITY COMPLEXES

a) Band degeneracy and stability of complexes

According to the shell model, the maximum number of electrons and holes in the ground state of the complexes is determined by the degree of degeneracy of the conduction band and the valence band. It would therefore be natural to expect that a strong uniaxial deformation, which would lead to a partial lifting of the degeneracy, would have the consequence that complexes with a large number of bound excitons either would have a much lower binding energy or would not form at all. The effect of a strong uniaxial deformation on multiexciton–impurity complexes in silicon was first studied by Kulakovskiĭ.[19] At the deformation levels he used, the splitting of the valence band was much greater than the binding energy of the excitons in the complexes, so that only those states corresponding to the lower split-off band could be occupied. Under these conditions the degeneracy of the valence band is two. The conduction band remains at least fourfold degenerate, since the valleys lying on a common axis are not split. Consequently, in multiexciton–impurity complexes at donors and acceptors in deformed silicon, the first shell to be filled is a hole shell which can hold only two holes. Measurements have shown that in Si(B) and Si(P) subjected to a large deformation along any of the axes ⟨111⟩, ⟨110⟩, and ⟨100⟩ the emission lines of complexes having three and four holes disappear. The only emis-

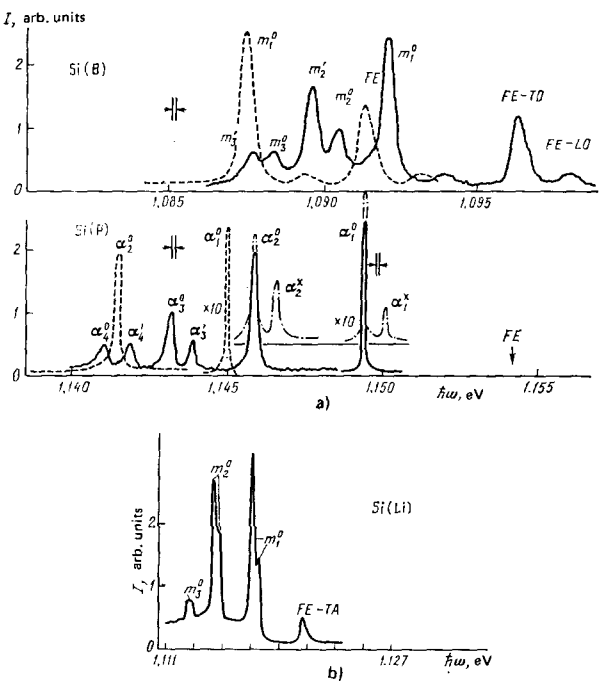

FIG. 9. Emission spectra of multiexciton–impurity complexes in uniaxial compressed silicon doped with B, P, and Li. a—Si(B) and Si(P), with pressure exerted in the direction P‖⟨111⟩ at $T = 1.8$ K. Solid curve) $P = 20$ MPa; dashed curve) $P = 120$ MPa; dot-dashed curve) $P = 20$ MPa at $T = 7$ K (Ref. 19); b—Si(Li), P‖⟨100⟩, $P = 175$ MPa, $T = 1.6$ K (Ref. 30).

sion lines which remain in the case of Si(P) are those which correspond to the recombination of e-h pairs in complexes with one or two excitons; the same is true of Si(B), except that the complexes must have only one exciton (Fig. 9). Corresponding results were subsequently obtained in a study of the stability of complexes at various donors (P, As, Sb) and acceptors (B, Al) (Refs. 26, 30, and 34). In all cases it was found that the emission lines of complexes having three holes disappear from the spectrum at 2 K if their binding energy falls below 1 meV. The formation of complexes having such a low energy is obviously not a thermodynamically favored process.

The situation is slightly different in highly compressed Si(Li), in which the only remaining emission line is that corresponding to a complex with three holes.[30] In Si(Li) the electron ground state is not the Γ_1 spin singlet but the tenfold degenerate $\Gamma_{3,5}$ state. Consequently, the binding energy of NDE_3 (four electrons and three holes) in Si(Li) is 1.5 times that in Si(P). Under these conditions, NDE_3 remains stable even in highly compressed silicon, despite the fact that it includes a hole in an excited state, as in a multiexciton–impurity complex with five holes in undeformed silicon. The exciton binding energy in NDE_3 in strongly compressed Si(Li) is only one-fourth that in the undeformed crystal, while the binding energy of complexes with one and two holes remains essentially constant. These experimental results confirm that an orbital degeneracy of the bands is a necessary condition for the formation of bound multiexciton–impurity complexes with $m > 1$. When the band degeneracy permits the formation of a complex with two or more excitons, in which all the electrons and holes are in the 1s ground state, the possibility that yet another exciton with an excited hole will be bound to such a complex increases with increasing band degeneracy. In highly compressed silicon, for example, complexes with three holes form only in Si(Li), while in undeformed silicon complexes with five holes form at all donors and acceptors.

Valuable information on the electron states of the complexes can be found by studying the splitting of the emission lines of multiexciton–impurity complexes with a slight uniaxial deformation, such that the band splittings Δ_{cc} and Δ_{cv} are smaller than the exciton binding energy in the complexes. As mentioned earlier, in the first studies in this direction[8,45] it was found that all the m_m lines in Si(B) and α_m lines in Si(P) split into the same number of components as the emission lines of exciton–impurity complexes, m_1 and α_1, respectively. In the one-electron approximation, which is the basis for the shell model, this result can be explained naturally, since the shift of each of the lines is determined by only the change in the energy of the recombining pair and does not depend on changes in the energy of other electrons or holes.[15,18] The relationships between the densities of the components should change from line to line, since the numbers of electrons and holes occupying the corresponding states change with increasing number of e-h pairs in the multiexciton–impurity complexes. This effect can be seen particularly well in level splittings greater than kT: In multiexciton–impurity complexes with few excitons, only the low-lying levels are filled under these conditions, while as the number of bound pairs increases there is a filling of levels with high energies. The splitting of the α lines in Si(P) and of the m lines in Si(B) has been studied in detail.[19,30,34]

b) Splitting of bands of levels of a free exciton and of shallow impurities in deformed silicon

In the multivalley semiconductors Si, Ge, and SiC, the extent to which the conduction band splits depends on the direction of the deformation, **P**, while the fourfold-degenerate valence band ($J = 3/2$) always splits into two twofold-degenerate subbands. The energy of these bands at the extremum ($K = 0$) is given by[16]

$$E = \pm\sqrt{\mathscr{E}_v} = \pm\sqrt{\frac{b^2}{2}[(\varepsilon_{xx}-\varepsilon_{yy})^2+(\varepsilon_{xx}-\varepsilon_{zz})^2+(\varepsilon_{yy}-\varepsilon_{zz})^2]+d^2(\varepsilon_{xy}^2+\varepsilon_{xz}^2+\varepsilon_{yz}^2)}. \quad (19)$$

For deformation along the ⟨100⟩ or ⟨111⟩ principal axes, the split levels correspond to states with $j_z = \pm 3/2$ and $\pm 1/2$. During compression, the lower level for holes is the ($\pm 1/2$) level, while during extension this lower level is ($\pm 3/2$). For deformation along other directions, the split states cannot be assigned a definite angular momentum projection j_z onto the deformation direction, although these states are frequently called $j_z = \pm 3/2$ or $\pm 1/2$ states for brevity. At hole kinetic energies comparable to the magnitude of the deformation splitting, the magnitude of the deformation shift and the value of j_z depend on the direction of the quasimomentum during compression along any axis.

The conduction band in silicon is not split in the case P ‖⟨111⟩, but with P ‖⟨100⟩ and P ‖⟨110⟩ it splits in two. The number of valleys in the lower band is two if the compression is along the ⟨100⟩ axis. For other deformation directions, there is a splitting into three bands. In germanium the conduction band does not split with P ‖⟨100⟩; with P ‖⟨111⟩ and P ‖⟨110⟩, there is a splitting in two; for other directions, there is a splitting into three or four bands. The splitting of a free-exciton level results from a splitting of both the conduction band and the valence band; the contributions are additive.[16] The level of a free exciton in silicon thus splits in two with P‖⟨111⟩ or in four with P ‖⟨100⟩ or ⟨110⟩ (Ref. 46). At small deformations we should expect a crystal splitting of the hole states of a free exciton. This splitting can be described by introducing the initial deformation ε_0 in (19), directed along the principal axis of the corresponding extremum: (100), (010), (001) in silicon and (111), (11$\bar{1}$), (1$\bar{1}$1), and ($\bar{1}$11) in germanium. In silicon, with a small crystal splitting (~0.3 meV; Ref. 41), the splitting is seen only at a very small load ($\lesssim$ 10 MPa), at which a nonlinearity is observed in the shifts of the split levels of the free exciton. In germanium, the crystal splitting is[40] ~1 meV.

In multiexciton–impurity complexes at donors, the electrons occupy the states of a neutral donor. The splitting of the 1s ground state of the neutral donor has been studied well (see Ref. 16, for example). In a description of the deformation depenedence of the energy

levels, the lowering of the symmetry of the impurity center in the deformed crystal can be ignored in a first approximation, and the valley-orbit splitting can be assumed independent of the deformation. In this case the matrix of the interaction with the deformation for silicon is[16]

$$
\begin{array}{c}
\Gamma_1 \\ \Gamma_3 \\ \\ \\ \Gamma_5 \\ \\ \\
\end{array}
\left|
\begin{array}{cccccc}
\frac{1}{3}(E_1+E_2+E_3) & \frac{1}{\sqrt{6}}(E_1-E_2) & -\frac{1}{3\sqrt{2}}(2E_3-E_1-E_2) & 0 & 0 & 0 \\
\frac{1}{\sqrt{6}}(E_1-E_2) & \frac{1}{2}(E_1+E_2)+\Delta_3 & \frac{1}{2\sqrt{3}}(E_1-E_2) & 0 & 0 & 0 \\
-\frac{1}{3\sqrt{2}}(2E_3-E_1-E_2) & \frac{1}{2\sqrt{3}}(E_1-E_2) & \frac{1}{6}(E_1+E_2)+\frac{2}{3}E_3+\Delta_3 & 0 & 0 & 0 \\
0 & 0 & 0 & E_1+\Delta_5 & 0 & 0 \\
0 & 0 & 0 & 0 & E_2+\Delta_5 & 0 \\
0 & 0 & 0 & 0 & 0 & E_3+\Delta_5
\end{array}
\right|, \tag{20}
$$

where E_i is the shift of the valley on the axis $i = x, y, z$; Δ_3 and Δ_5 are the valley–orbit splittings for the Γ_3 and Γ_5 terms in undeformed silicon. With $\mathbf{P}\parallel\langle 111\rangle$, and $E_1 = E_2 = E_3$, there is no splitting of the Γ_3, Γ_5, and Γ_1 levels. With $\mathbf{P}\parallel\langle 100\rangle$ or $\mathbf{P}\parallel\langle 110\rangle$, the conduction band splits in two: a fourfold-degenerate band and a twofold-degenerate one. In the first case we have $E_1 = -\frac{2}{3}\Delta_{cc}$, $E_2 = E_3 = \frac{1}{3}\Delta_{cc}$; in the second we have $E_1 = E_2 = -\frac{1}{3}\Delta_{cc}$ and $E_3 = (2/3)\Delta_{cc}$, where Δ_{cc} is the deformation splitting of the conduction band ($\Delta_{cc} > 0$ for compression and $\Delta_{cc} < 0$ for extension). According to (20), the state of a neutral donor splits into five levels. If $\Delta_3 = \Delta_5$, two of these levels are coincident. The number of split levels which derive from the Γ_5 term during deformation along the $\langle 111\rangle$ and $\langle 110\rangle$ directions (Fig. 10) is lower than allowed by group theory (Table IV). The reason is that expression (20) ignores the change in the valley–orbit splitting upon deformation. This change is small and can essentially always be ignored.

We turn now to a neutral acceptor, whose Γ_8 ground state in undeformed silicon and germanium is fourfold degenerate in the spin. Deformation along any axis splits this state, like the valence band, into two twofold-degenerate states. This splitting is determined by Eq. (19). The splitting of the ground state of a neutral acceptor is slightly smaller than the band splitting at the point $K = 0$.

TABLE IV. Splitting of the Γ_1, Γ_3, Γ_5, and Γ_8 states in silicon deformed along various axes.

Deformation direction	Symmetry	States			
No deformation	T_d	Γ_1	Γ_3	Γ_5	Γ_8
$\langle 111\rangle$	C_{3v}	Γ_1	Γ_2	$\Gamma_1+\Gamma_3$	$\Gamma_4+\Gamma_5+\Gamma_6$
$\langle 110\rangle$	C_{2v}	Γ_1	$\Gamma_1+\Gamma_3$	$\Gamma_1+\Gamma_2+\Gamma_4$	$\Gamma_3+\Gamma_5$
$\langle 100\rangle$	D_{2d}	Γ_1	$\Gamma_1+\Gamma_3$	$\Gamma_4+\Gamma_5$	$\Gamma_6+\Gamma_7$

c) Splitting of the levels of multiexciton–impurity complexes in silicon deformed along the ⟨111⟩ axis

According to the shell model, the electrons and holes in the complexes successively occupy the neutral-impurity states discussed above. The pattern of level splitting is simplest in the case $\mathbf{P}\parallel\langle 111\rangle$ (Fig. 12), in which case the electron states do not split. It can be seen from Fig. 11 that all the α lines in Si(P) and all the m lines in Si(B) with $\mathbf{P}\parallel\langle 111\rangle$ split into doublets. This result means that the splitting of the hole shells is the same, $\Delta_m^h \approx \Delta^h$, for all complexes at P and B with $m \geq 1$. At a fixed temperature, the population of the upper levels of the complexes falls off with increasing Δ^h. At thermodynamic equilibrium, the intensity ratios of the doublet components for complexes containing n_h holes are described by

$$
\left.
\begin{array}{ll}
n_h = 1: & \frac{I'}{I} = \exp\left(-\frac{\Delta^h}{kT}\right), \\
n_h = 2: & \frac{I'}{I} = \frac{4\exp(-\Delta^h/kT)+\exp(-2\Delta^h/kT)}{1+4\exp(-\Delta^h/kT)}, \\
n_h = 3: & \frac{I'}{I} = \frac{1+2\exp(-\Delta^h/kT)}{2+\exp(-\Delta^h/kT)}, \\
n_h = 4: & \frac{I'}{I} = 1.
\end{array}
\right| \tag{21}
$$

The measurements of $I'/I(\Delta^h)$ at a fixed temperature in Si(B), Si(P) (Refs. 19, 30, and 34), and Si(Li) (Ref. 30) agree well with the results expected on the basis of the

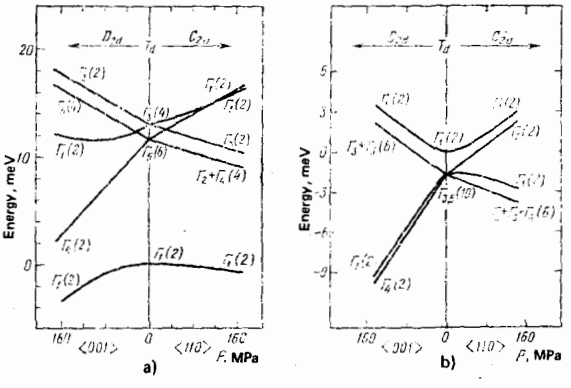

FIG. 10. Splitting of the 1s state of a neutral donor in silicon for compressions $\mathbf{P}\parallel\langle 100\rangle$ and $\mathbf{P}\parallel\langle 110\rangle$. a—Si(P); b—Si(Li). The degeneracy of the term is given in parentheses.

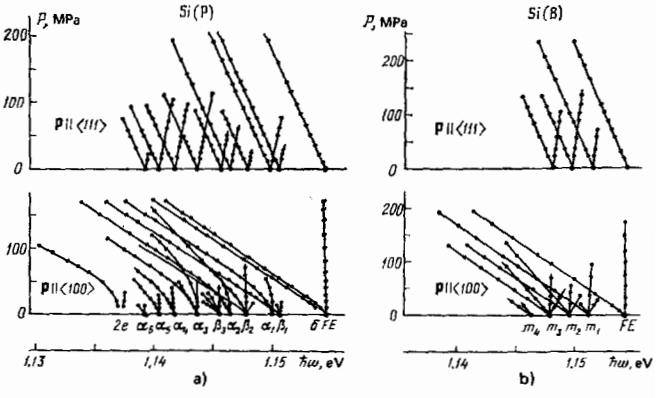

FIG. 11. Splitting of the lines of multiexciton–impurity complexes in Si(P) and Si(B) during compression along the ⟨100⟩ and ⟨111⟩ directions.[19,30,48] For convenience in comparison of the spectra, the β lines in Si(P) and the free-exciton (FE) lines in Si(B) and Si(P), meansured in the phonon region, are shifted by the energy of the TO phonon (58.05 meV) into the no-phonon part of the spectrum.

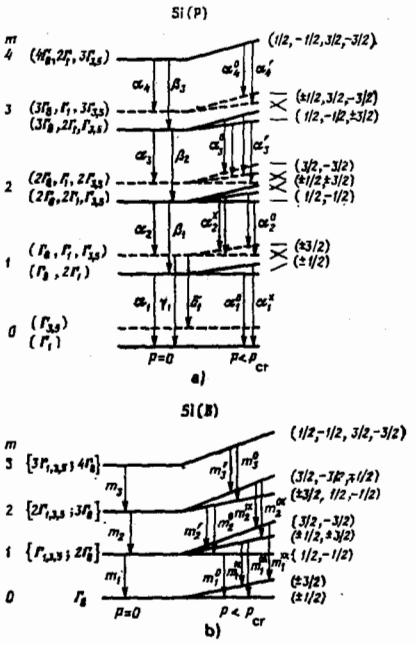

FIG. 12. Diagram of allowed optical transitions between the levels of multiexciton–impurity complexes during a slight deformation along the ⟨111⟩ axis. a—Si(P); b—Si(B). The splitting of the β lines in Si(P) is not shown.

shell model. For the α_5 and α_6 lines in Si(P) and the m_4 line in Si(B), the ratio I'/I is unity, as for α_4 and m_3 (Ref. 25). This result shows that the α_5, α_6, and m_4 lines result from the recombination of holes from the Γ_8 ground state, as has been suggested previously.[15,18]

With increasing deformation, the absolute intensities of the emission lines of complexes having one and two holes increase slightly in both Si(P) and Si(B), while the intensities for complexes having three or more holes fall off, and the lines vanish completely at $P > P_{cr} \sim 120$ MPa (Ref. 19). From the position of the β_2' and β_3' lines in Si(P) and the m_2' and m_3' lines in Si(B), which correspond to transitions to the ground states, we can follow the change in the exciton binding energy in multiexciton–impurity complexes with $n_h = 3$ and 4, respectively. Extrapolation of the positions of these lines to $P = P_{cr}$ in Si(P) and Si(B) leads to an exciton binding energy ~1 meV in complexes with $n_h = 3$ and ~3 meV in complexes with $n_h = 4$. The disappearance of the complexes with $n_h = 3$ at $P \sim P_{cr}$ is therefore caused by thermal dissociation.[19,30] The absence of these complexes also leads to the disappearance of multiexciton–impurity complexes with $n_h = 4$, since the probability for the simultaneous capture of two excitons to a complex is vanishingly small in comparison with the lifetime of such complexes. In accordance with the significantly larger binding energy of complexes with $n_h = 4$, the intensity ratio of the α_4 and α_3 lines in Si(P) and that of the m_3 and m_4 lines in Si(B) depend only slightly on the deformation up to $P \sim P_{cr}$.

d) Effect of the splitting of the conduction band

As mentioned earlier (Fig. 10), the Γ_1 state remains a singlet upon deformation along any axis, so that the α_m emission lines in Si(P) for P ‖⟨100⟩ and ⟨110⟩, as in the case P ‖⟨111⟩, are split into only two components, because of the splitting of the hole shell. Additional components appear only for the lines which result from the recombination of $\Gamma_{3,5}$ electrons, i.e., the β lines in Si(P) and all the lines in Si(Li) and Si(B). Since $\Gamma_{3,5}$ splits into the three subshells[4)] Γ_4^5, Γ_1^3, and $\Gamma_{3,5}^{3,5}$ in the case P ‖⟨100⟩, the number of components in the β lines can reach six, when the twofold splitting of the hole shell is taken into account. Although the β lines also have a large half-width in this (phonon) part of the spectrum, there are intense α lines, most of whose components can be resolved.[30,47] Let us examine the main aspects of the behavior of the β lines in compressed Si(P). For very large deformations P ‖⟨100⟩, the emission spectrum retains only a single component of the NDE_2 emission line, β_1, which corresponds to the $\{2\Gamma_1^1, \Gamma_4^5; 2\Gamma_6^8\} \to \{2\Gamma_1^1; \Gamma_6^8\}$ transition and which is seen only in the phonon part of the spectrum.[19,30] For a small deformation in the phonon region, we can distinguish four components in each of the lines β_2 of NDE_3 and β_3 of NDE_4; in each case, two of the components (the fainter ones) are also seen in the no-phonon spectrum.[30] This aspect of the β_2 and β_3 lines can be explained easily by referring to the arrangement of states of a neutral donor (Fig. 10). Those components which are not found in the no-phonon spectrum result from the recombination of electrons in the Γ_4^5 state, while the components which are observed in the no-phonon spectrum result from the recombination of electrons from a higher term, Γ_1^3 (Refs. 30 and 34).

As mentioned in Section 3, the lines corresponding to the recombination of the Γ_3 and Γ_5 electrons have a very low intensity in the no-phonon spectrum. For deformation along ⟨100⟩ (and also along ⟨110⟩), the Γ_1^1 and Γ_1^3 states are mixed, with the result that the γ line intensifies. At large deformations, at which the deformation splitting Δ_{tc} is much greater than the valley–orbit splitting, the wave function of the Γ_1^3 electrons is a symmetrized combination of the wave functions of the four upper valleys, while the Γ_1^1 wave function is a symmetrized combination of the wave functions of the two lower valleys.

The presence of the Γ_1^3 electron state, symmetric with respect to the valleys, in deformed silicon also leads to the intensification of the $2e$ line, which corresponds to two-electron transitions[30,48] $\{2\Gamma_1^1(1s); \Gamma_6^8\} \to \{\Gamma_1^3\}$ (Fig. 12). The ratio of the intensity of the $2e$ line to that of the α_1 line, which corresponds to a transition from the same state of the exciton–impurity complex, does not depend on the excitation density or the temperature, and the difference $\hbar\omega(\alpha_1) - \hbar\omega(2e)$ (Fig. 11) corresponds well to the splitting of the Γ_1^1 and Γ_1^3 states which has been found for the phosphorus neutral donor (Fig. 10a). The transitions from $\{2\Gamma_1^1; \Gamma_6^8\}$ to the antisymmetric Γ_4^5 and Γ_1^3 states and also the transition from $\{2\Gamma_1; \Gamma_6\}$ to $\Gamma_{3,5}$ are not observed in undeformed silicon. In Si(Li) compressed along the ⟨100⟩ axis, the splitting of the Γ_4^5 and Γ_1^3 lower terms (Fig. 10b) in NDE_m is slight even at a

[4)]The superscripts denote the states from which the given subshells derive.

large compression $P \gtrsim 100$ MPa $[E(\Gamma_4^5) - E(\Gamma_1^3) \sim 0.1$ meV]. Under equilibrium conditions, therefore, the upper level is occupied even at $T \approx 1.6$ K. The emission spectrum of Si(Li) compressed in this manner shows a doublet structure for the NDE_1 and NDE_2 lines at any pressure[30] (Fig. 9b).

e) "Hot" luminescence of multiexciton–impurity complexes

In addition to these transitions from the ground states of multiexciton–impurity complexes in Si(P) compressed along the ⟨100⟩ axis, even at 2 K we can clearly see emission lines corresponding to transitions from an excited state of an exciton–impurity complex, $\{\Gamma_1^1, \Gamma_4^5, \Gamma_6^8\}$, in Γ_1^1 (the δ transition) and in Γ_4^5 (the γ transition).[30,34] In undeformed silicon these lines appear only at[18] $T > 15$ K. The ratio $I(\delta)/I(\gamma)$ does not depend on the excitation intensity or the temperature. One reason for the intensification of these lines is the decrease in the splitting of these states, from 4 meV in undeformed silicon to 1.5 meV in highly compressed silicon. Even with the splitting, however, the fraction of exciton–impurity complexes which are excited at 2 K at thermodynamic equilibrium should be vanishingly small. In all probability the relaxation time increases upon deformation and becomes comparable to the lifetime of the state. A significant deviation from a thermodynamic-equilibrium distribution is also observed for complexes with $m > 1$ containing electrons from $\Gamma_{3,5}$ excited states in addition to the Γ_1^3 term.[30] The relaxation times of electrons in such complexes have not been calculated.

The most pronounced deviation from a thermodynamic-equilibrium state is observed in complexes at acceptors (B, Al) (Fig. 13; Refs. 19, 20, and 30), in which case the electron wave function at the impurity center is small in all states, so that it is difficult for momentum to be transferred to the impurity. In relatively pure Si(B) crystals, with an impurity concentration $\sim 10^{13}$ cm^{-3}, for example, the emission line of a "hot" exciton–impurity complex at a boron atom is visible at 2 K at a splitting of the conduction band greater than 10 meV (Refs. 19 and 49). The shift of the m_1' and $m_1(c)$ lines in Si(B) is linear in the deformation (Fig. 11), showing that there is essentially no valley–orbit splitting of the Γ_1 and $\Gamma_{3,5}$ states in multiexciton–impurity complexes in undeformed Si(B), as we would expect in the case of an acceptor center.

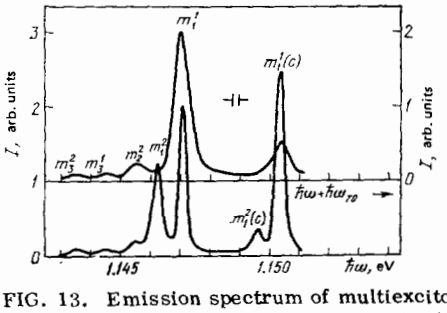

FIG. 13. Emission spectrum of multiexciton–impurity complexes in Si(Al) compressed along the ⟨111⟩ axis ($T = 1.8$ K; Ref. 20). Top—The TO components; bottom—the no-phonon region. The emission lines of NAE_1 with an electron in the upper split-off valey are denoted by "C". The lines are classified in accordance with the transition scheme in Fig. 14b.

f) Level splitting in the case of strong j-j coupling

As mentioned in Section 2, the two-hole $\Gamma_8 \times \Gamma_8$ state splits into the three terms Γ_1, Γ_3, and Γ_5 in exciton–impurity complexes at acceptors deeper than boron. In the absence of a splitting of the Γ_3 and Γ_5 terms, in which case these five levels form a state with a total angular momentum $J = 2$ and with $J_z = \pm 2, \pm 1, 0$, deformation causes a mixing of the states with $J_z = 0$ and the terms with $J = 0$ and $J = 2$ (for deformation along the ⟨100⟩ and ⟨111⟩ axes, the z axis is directed along the corresponding axis). The energy of these states is[50,51]

$$E_{1,2} = -\frac{1}{2}\Delta_{ex} \pm \sqrt{\Delta_{ex}^2 + 4\Delta_{cv}^2}; \tag{22}$$

where Δ_{ex} is the exchange splitting, and the deformation splitting Δ_{cv} is given by $\Delta_{cv} = 2\sqrt{\mathscr{E}_c}$, where $\mathscr{E}_c$ is given by Eq. (19). The energies of the other terms with $J = 2$ do not change. If the exchange splittings of the $\Gamma_5 - \Gamma_1(\Delta_{ex})$ and $\Gamma_3 - \Gamma_1(\Delta_{ex}')$ terms are different, then each of the Γ_5 and Γ_3 states will, in general, split into two levels upon deformation in an arbitrary direction. If the deformation is along the ⟨100⟩ axis, only the Γ_3 level splits; if the deformation is along the ⟨111⟩ axis, only Γ_5 splits. The energies of the two levels, which depend on the deformation, are found from Eq. (22); in the first case, Δ_{ex} should be taken as the distance to the Γ_3 level, i.e., Δ_{ex}', while in the second case it should be taken as the distance to the Γ_5 level (Δ_{ex}). If there is a significant crystal splitting, in addition to the external deformation we should take into account the internal strain along the axis of the corresponding extremum.

All the transitions for multiexciton–impurity complexes at acceptors which are allowed in highly deformed crystals as one-electron complexes (the solid arrows in Fig. 14b), can be seen well in the emission spectra of Si(Al) (Fig. 14a; Ref. 20). The transitions

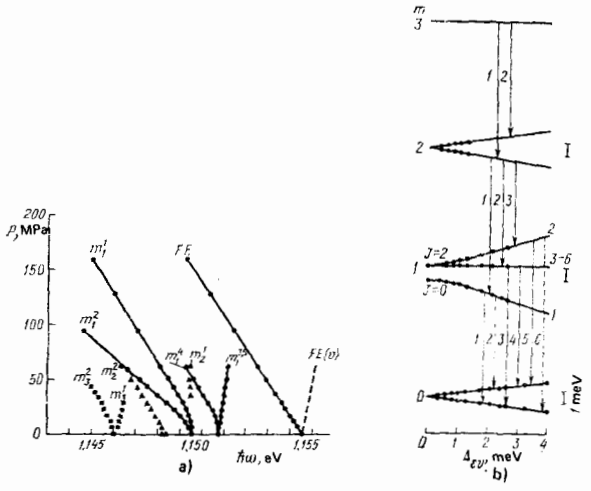

FIG. 14. Splitting of the emission lines of multiexciton–impurity complexes in Si(Al) compressed along the ⟨111⟩ axis.[20] a—Observed splitting; b—splitting scheme. The dots show the measured level splittings.

indicated by the dashed arrows in Fig. 14b are allowed only at small deformations, because of a mixing of different one-particle wave functions in the E_1 and E_2 states by the exchange interaction. For deformation along the ⟨100⟩ and ⟨111⟩ axes, the intensities of these lines should fall off with increasing deformation in accordance with

$$\frac{I_f(\Delta_{\varepsilon v})}{I_f(0)}=1-\frac{\Delta_{\varepsilon v}}{\sqrt{\frac{1}{4}\Delta_{\varepsilon x}^2+\mathscr{E}_\varepsilon}}, \tag{23}$$

while the intensity of the allowed lines should rise slightly,

$$\frac{I_a(\Delta_{\varepsilon v})}{I_a(0)}=1+\frac{\Delta_{\varepsilon v}}{\sqrt{\frac{1}{4}\Delta_{\varepsilon v}^2+\mathscr{E}_\varepsilon}}. \tag{24}$$

For deformation along an axis other than ⟨100⟩ and ⟨111⟩, the split hole states do not have a definite angular momentum, and Eqs. (23) and (24) hold only under the isotropy condition

$$\frac{2b}{c_{11}-c_{12}}=\frac{d}{\sqrt{3}c_{44}}. \tag{25}$$

For silicon, we have

$$\frac{2b}{c_{11}-c_{12}}\frac{\sqrt{3}c_{44}}{d}\approx 1{,}14,$$

so that the deviation from (24), (23) should be slight. The m_1^2 emission line of an exciton–impurity complex which corresponds to transition 2 and which lies on the red side of the m_1^1 emission line, separated from it by an amount equal to the splitting of the neutral-acceptor level, can be seen clearly in the no-phonon spectrum in Fig. 13. It cannot, however, be followed in the phonon repetitions.[20] Figure 15 shows the dependence of the intensity ratio of the no-phonon lines m_1^2 and m_1^1 for P‖⟨100⟩, ⟨110⟩, and ⟨111⟩, along with the result calculated from Eqs. (23) and (24), for two values of the constants d and b measured for NAE_1 and a neutral acceptor. It can be seen from this figure that the experimental dependence $I(m_1^2)/I(m_1^1)$ for "cold" exciton–impurity complexes in Si(Al) compressed along the ⟨100⟩ axis is much weaker than in other cases. This behavior implies a significant deviation from the shell model.

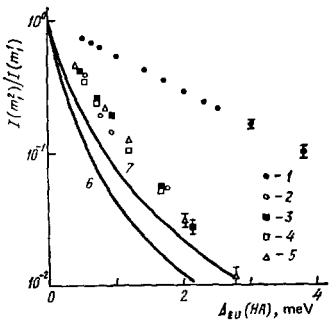

FIG. 15. Dependence of the intensity ratios of the m_1^2 and m_1^1 lines of multiexciton–impurity complexes in Si(Al) on the magnitude of the splitting of the ground state of the neutral acceptor. The experimental values were obtained under the following conditions: 1—P‖⟨100⟩, "cold" NAE_1; 2—P‖⟨100⟩, "hot" NAE_1; 3—P‖⟨110⟩, "cold" NAE_1; 4—P‖⟨110⟩, "hot" NAE_1; 5—P‖⟨111⟩. The solid curves are calculated for the parameter values $d/d_{FE}=b/b_{FE}=0.6$ (curve 6) and 0.8 (curve 7).

From the splitting of the emission lines we can determine the constants of the strain energy for holes in all multiexciton–impurity complexes in Si(B) and Si(Al), which determine the line splitting upon deformation along ⟨111⟩ or ⟨100⟩:

$$\Delta_{\varepsilon 111}=\frac{d_m}{\sqrt{3}}\varepsilon_{111}, \tag{26}$$

$$\Delta_{\varepsilon 100}=b_m\varepsilon_{100}. \tag{27}$$

Here ε_{111} and ε_{100} are the strains during deformations P‖⟨111⟩ and ⟨100⟩, respectively, and m is the number of excitons in the complex. As expected (Section 3), the values of $d_m(b_m)$ in a NAE_m at boron do not depend on the number of bound excitons and have the values ~0.84 $d_{FE}(b_{FE})$, as for a boron neutral acceptor.[20,52] For the deeper aluminum acceptor, we have[52] $d_{HA}(b_{HA})\approx 0.6\,d_{FE}(b_{FE})$. For a NAE_1 at aluminum, on the other hand, the deformation constants $d_1(b_1)$ increase to 0.8 $d_{FE}(b_{FE})$. *These constants do not change with a* further increase in the number of excitons in the NAE_m.

g) Polarization of the emission lines of multiexciton–impurity complexes in deformed silicon

According to the shell model, the polarization of each emission line of a multiexciton–impurity complex and also the spectral position of this line are determined by the states of the recombining electron and hole. Uniaxial deformation changes the energies of these states and the splitting of the corresponding emission lines. As mentioned above, in the simple case with P‖⟨111⟩, in which only the valence band is split, all the emission lines of multiexciton–impurity complexes split into doublets. The components of a doublet are conveniently denoted as X_f^a, where the superscript and the subscript specify the states of the recombining electron and hole, respectively (Fig. 16). We wish to call attention to the fact that during compression the $X_{\pm 1/2}^a$ lines are the longer-wavelength lines, while during extension the $X_{\pm 3/2}^a$ lines are the longer-wavelength lines. With P‖⟨100⟩, the electron states also split (Fig. 19), leading to a further splitting of the emission lines. The exciton emission lines thus split into two doublets, $FE_{\pm 1/2}^{(100)}$, $FE_{\pm 1/2}^{(001)(010)}$ and $FE_{\pm 3/2}^{(100)}$, $FE_{\pm 3/2}^{(001)(010)}$.

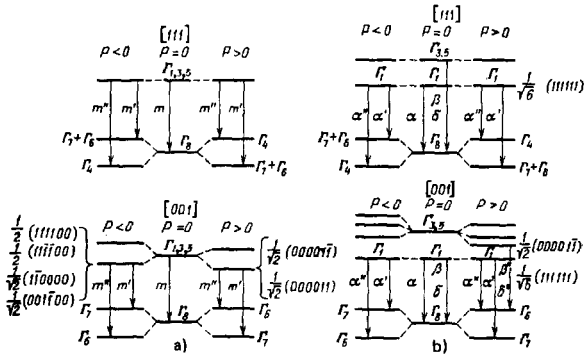

FIG. 16. One-electron transitions in a multiexciton–impurity complex at a substitution acceptor and at a substitution donor for the cases of uniaxial extension ($P<0$) and uniaxial compression ($P>0$) along the ⟨111⟩ and ⟨100⟩ axes.[55] a—Multiexciton–impurity complex at an acceptor, B; b—multiexciton–impurity complex at a donor, P.

TABLE V. Relative intensities of the TO and TA emission lines in deformed silicon in the π and σ polarizations.

P	Term	I^{π}	I^{σ}	For $\alpha/\beta=0.5$	
				I^{π}	I^{σ}
⟨111⟩	$X^{\Gamma_{1,3,5}}_{\pm 1/2}$	$2(\alpha^2+\alpha\beta+\beta^2)$	$2(\alpha^2+\beta^2)-\alpha\beta$	3.5	2.0
	$X^{\Gamma_{1,3,5}}_{\pm 3/2}$	$2(\alpha^2-\alpha\beta+\beta^2)$	$2(\alpha^2+\beta^2)+\alpha\beta$	1.5	3.0
⟨100⟩	$X^{(100)}_{\pm 1/2}$	α^2	$2\beta^2$	0.25	2
	$X^{(100)}_{\pm 3/2}$	$3\alpha^2$	0	0.75	0
	$X^{(010)(001)}_{\pm 1/2}$	β^2	$\frac{1}{2}(5\alpha^2+\beta^2)$	1	1.125
	$X^{(010)(001)}_{\pm 3/2}$	$3\beta^2$	$\frac{3}{2}(\alpha^2+\beta^2)$	3	1.875

As mentioned above, during the recombination of electrons and holes in multiexciton–impurity complexes involving phonons we should sum the intensities for transitions from different valleys. Table II shows selection rules for transitions associated with the recombination of Γ_1 and $\Gamma_{3,5}$ electrons with a Γ_8 hole for the TO (TA) lines. The results in this table can be used to calculate the relative intensities of the TO (TA) emission lines of free excitons in deformed silicon[25,53] (Table V). It follows from experimental work on the polarization of the exciton emission lines during uniaxial deformation of silicon[53] and during the imposition of a magnetic field[54] that we have a ratio $\alpha/\beta=0.5$ for the TO line. The numerical values of the transition intensities in this case are also listed in Table V.

The situation is simplest for multiexciton–impurity complexes in Si(B), for which there is no valley–orbit splitting of the 1s electron shell. As a result, the electron states split in accordance with the valley splitting.

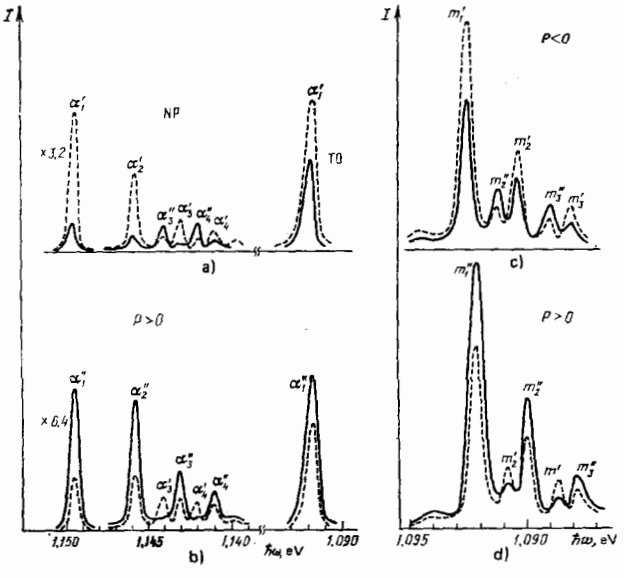

FIG. 17. Emission spectra of multiexciton–impurity complexes in the polarization parallel to the deformation direction P‖⟨111⟩ (solid curves) and in the direction perpendicular to the deformation direction (dashed curves), (Ref. 55). a,b—Si(P), $P=25$ MPa, $T=2$ K; c,d—Si(B), $P=22$ MPa, $T=2$ K; a,c—extension ($P<0$); b,d—compression ($P>0$).

TABLE VI. Degree of polarization of the emission lines of multiexciton–impurity complexes in uniaxially deformed silicon (+ — compression; - —extension).

Impurity	Deformation		Phonon	Line	State of recombining particles		Degree of polarization			
								Experimental		
	Direction	Sign			Electron	Hole	Calculated	Measured	Corrected	Exciton line FE (TO)
P	⟨111⟩	−	NP	α_1	Γ_1	±3/2	−100	−70	−100 *)	
		+	NP	α_1	Γ_1	±1/2	60	45	64	
	⟨100⟩	−	NP	α_1	Γ_1	±3/2	−100	−62	100 *)	
		+	NP	α_1	Γ_1	±1/2	60	42	66	
	⟨111⟩	+	TO	α_l	Γ_1	±1/2	27	19	27	
		−	TO	α_l	Γ_1	±3/2	−33	−23	−33	
	⟨100⟩	Slight compression	TO	α_l	Γ_1	±1/2	−43	−31	−49	
		Strong compression	TO	α_l	Γ_1	±1/2	−78	−50	−79	
		+	TO	β, δ	$\Gamma_{3,5}$	±1/2	−78	−50	−79	
		−	TO	α_l	Γ_1	±3/2	33	20	33	
B	⟨111⟩	+	TO	m_1	$\Gamma_{1,3,5}$	±1/2	27	19	27	24
		+	TO	m_2	$\Gamma_{1,3,5}$	±1/2	27	17	24	24
	⟨100⟩	+	TO	m_1	(100)	±1/2	−78	−47	−72	−68
		+	TO	m_2	(100)	±1/2	−78	−41	−65	−68
		−	TO	m_1	(010) (001)	±3/2	23	17	26	27
		−	TO	m_2	(010) (001)	±3/2	23	18	27	27

*Values used for determining the depolarization factor.

As we would expect in this case, the polarization of the phonon components of the emission lines of multiexciton–impurity complexes in Si(B) is the same as the polarization of the corresponding emission lines of free excitons[55] (Figs. 17c and 17d and Table VI).

In Si(P) the Γ_1 electron ground state for a deformation P‖⟨111⟩ incorporates in an identical fashion the wave functions of all six of the unsplit valleys. Consequently, the measured polarization of the phonon repetitions of the emission lines of exciton–impurity complexes is also the same as the polarization of the corresponding exciton lines.[55]

For deformations P‖⟨100⟩, the valleys in the conduction band are not equivalent. The valley–orbit interaction mixes the states of different valleys, and this mixing is seen in two terms:

$$E_{1,2}=\frac{1}{2}\left[\left(-\frac{1}{3}\Delta_{\varepsilon c}+\Delta_{VO}\right)\pm\sqrt{\Delta_{\varepsilon c}^2+\Delta_{VO}^2+\frac{2}{3}\Delta_{\varepsilon c}\Delta_{VO}}\right]. \quad (28)$$

The polarization of the corresponding emission lines of the corresponding emission lines of multiexciton–impurity complexes at donors thus depends on the ratio of the deformation splitting $\Delta_{\varepsilon c}$ and the valley–orbit splitting Δ_{VO}. The intensities of these lines (the populations are not taken into account) in the π and σ polarizations are given by

$$I^{\pi(\sigma)}_{E_1}=\frac{1}{6(1+2\zeta^2)}\left[4I^{\pi(\sigma)}(FE^{(100)}_{3/2(1/2)})(1-\zeta)^2+I^{\pi(\sigma)}(FE^{(010)(001)}_{3/2(1/2)})(1+2\zeta)^2\right], \quad (29)$$

$$I^{\pi(\sigma)}_{E_2}=\frac{1}{3(1+2\zeta^2)}\left[I^{\pi(\sigma)}(FE^{(100)}_{3/2(1/2)})(1+2\zeta)^2+I^{\pi(\sigma)}(FE^{(010)(001)}_{3/2(1/2)})(1-\zeta)^2\right], \quad (29')$$

where $\zeta\equiv\Delta_{\varepsilon c}/3E_1$.

The remaining four terms are formed either exclusively by electrons of the (100) valley ($E_3=\Delta_{VO}-\frac{2}{3}\Delta_{\varepsilon c}$) or by electrons of both the (010) and (001) valleys ($E_{4-6}=\Delta_{VO}+\frac{1}{3}\Delta_{\varepsilon c}$). The polarization of the emission lines corresponding to these terms should be the same as the polarization of the $FE^{(100)}_{3/2(1/2)}$ and $FE^{(001)(010)}_{3/2(1/2)}$ emission lines, respectively, and the relative intensities of these

lines should be one (E_3) and three (E_{4-6}).

It can be seen from (28) and (29) that with a small deformation, such that the mixing of the Γ_3 states into Γ_1 can be ignored, we have the following for the α line in Si(P):

$$I(\alpha_{3/2(1/2)}) = \frac{1}{3}[I(\mathrm{FE}^{(100)}_{3/2(1/2)}) + I(\mathrm{FE}^{(010)(001)}_{3/2(1/2)})]. \quad (30)$$

In other words, the intensity is equal to the sum of the intensities of the exciton transitions from different valleys. For a large deformation ($\zeta \to 1$) the lower electron state includes the wave functions of only the two lower valleys, and we have

$$I(\alpha_{3/2(1/2)}) \to I(\mathrm{FE}^{(100)}_{3/2(1/2)}). \quad (31)$$

Table VI shows the calculated and experimental degrees of polarization of the TO components of several lines in Si(P) (Ref. 55). Under the particular experimental conditions, the light leaving the crystal was partially depolarized by the multiple reflections in the crystal, so that a corresponding depolarization coefficient is introduced for convenience in comparing the calculated and experimental degrees of polarization. We determined this coefficient from the measured polarization of the no-phonon line, $\alpha^{\Gamma_1}_{1,3/2}$, which should be 100% according to the theory. As can be seen from Table VI, the introduction of this coefficient leads to good agreement between the calculated and experimental values for all lines.

Transitions in multiexciton–impurity complexes involving phonons were discussed above. As was mentioned above, a calculation of the intensities of no-phonon lines differs from a calculation for the phonon components in that there is an interference between transitions from different valleys. The relative intensities of the no-phonon transitions are the same during the recombination of Γ_1 electrons with deformations $\mathbf{P} \parallel \langle 100\rangle$ and $\mathbf{P} \parallel \langle 111\rangle$ (Table VII). It follows from Table VII that the degree of polarization for the $\alpha^{\Gamma_1}_{1,\pm 3/2}$ and $\alpha^{\Gamma_1}_{1,\pm 1/2}$ lines should be 100% and 60%, respectively. Figures 17a and 17b show experimental emission spectra[55] of multiexciton–impurity complexes in Si(P). As for the TO components, the agreement between the measured and calculated degrees of polarization is good when the depolarization factor is taken into account.

For deformation along directions other than $\langle 111\rangle$ and $\langle 100\rangle$, the intensities I^π and I^σ depend on the light propagation direction and also on the ratio of elastic moduli, $(s_{11} - s_{12})/s_{44}$, and the ratio of strain-energy constants b/d [these constants are determined from Eqs. (40) and (39) from Ref. 16, as for $\Gamma^1_2 - \Gamma_8$ direct transitions].

TABLE VII. Relative intensities of the NP lines α_m in deformed silicon in the π and σ polarizations for $\mathbf{P} \parallel \langle 100\rangle$ and $\mathbf{P} \parallel \langle 111\rangle$.

Term	I^π	I^σ
$X^a_{\pm 1/2}$	4	1
$X^a_{\pm 3/2}$	0	3

When there is j–j coupling (the cases of multiexciton–impurity complexes at Al, Ga, and In acceptors), the additional splitting of the two-hole state must be taken into account: $\Gamma_8 \times \Gamma_8 = \Gamma_1 + \Gamma_3 + \Gamma_5$. If the splitting of Γ_3 and Γ_5 is small enough, it may be ignored. A uniaxial deformation does not shift four of the five $\Gamma_3 + \Gamma_5$ levels having $J_z = \pm 2(\pm 1/2, \pm 3/2)$ and $J_z = \pm 1(\pm 1/2, \pm 3/2)$. The polarization of the $X^a_{\pm 1/2}$ and $X^a_{\pm 3/2}$ lines is the same as that of the corresponding emission lines of free excitons, $\mathrm{FE}^a_{\pm 1/2}$ and $\mathrm{FE}^a_{\pm 3/2}$. The resultant intensity of these lines is four.

The spin states of the two remaining levels (Fig. 14b), E_1 and E_2, are superpositions of the $\pm 1/2$ and $\pm 3/2$ states. Both of the lines corresponding to transitions from these states therefore split into doublets because of the splitting of the final state of the neutral acceptor. The polarization of the lower-energy lines in these doublets is the same as that of the short-wave component in the doublet which arises upon the recombination of holes in $J_z = \pm 2, \pm 1$ states which derive from $\Gamma_{3,5}$.

As the deformation becomes stronger, the contribution of the $\pm 3/2$ holes to E_1 and that of the $\pm 1/2$ holes to E_2 decreases, and the lines corresponding to recombination of holes in these states disappear from the spectrum. A strong deformation leaves only a pair of lines, which form a doublet split by an amount $2\Delta_{ce}$ and shifted from the E_{3-6} doublet by an energy $\Delta_{\mathrm{VO}}/2$. The arrangement of the lines in this doublet is the same as in the E_{3-6} doublet, while the relative intensity is only half as large (the level populations are not taken into account).

h) Binding energies of multiexciton–impurity complexes in deformed silicon

The binding energies of exciton–impurity complexes in Si(B) and Si(Li) remain constant, within the error in their determination (~0.2 meV), when the silicon crystals are deformed along any axis.[19,30] The situation is different in the case of Si(P). In undeformed Si(P) and also in Si(P) compressed along the $\langle 111\rangle$, $\langle 110\rangle$, and $\langle 100\rangle$ axes, the binding energies of the exciton–impurity complexes are $\delta_1 = 4.5$, $\delta_{1\langle 111\rangle} = 4.3$, $\delta_{1\langle 110\rangle} = 3.3$, and $\delta_{1\langle 100\rangle} = 2.9 \pm 0.2$ meV, respectively.[19] It can be seen from these values that Γ_1 changes markedly in those cases in which the deformation leads to a splitting of the conduction band and to a decrease of the chemical shift related to the valley–orbit interaction. According to (20), the chemical shift of the Γ^1_1 lower level in Si(P) should decrease by an amount $2\Delta_{\mathrm{VO}}/3$ in the case of a strong compression along the $\langle 100\rangle$ axis, and it should decrease by $\Delta_{\mathrm{VO}}/3$ for compression along the $\langle 110\rangle$ axis; here Δ_{VO} is the valley–orbit splitting in the undeformed crystal. As a result, the distance from the Γ^1_1 level to the nearest of the split $\Gamma_{3,5}$ levels decreases by a factor of three in the first case and by a factor of 1.5 in the second (the change in the smooth functions upon the deformation is not taken into account). There is a dif-

ference between the cases Si(Li) and Si(P) in that the chemical shift of the lower, multiply degenerate $\Gamma_{3,5}$ level in Si(Li) upon deformation along the ⟨100⟩ and ⟨110⟩ axes does not change [although the distance to the nearest levels also decreases by a factor of three (P‖⟨100⟩) or 1.5(P‖⟨110⟩), as mentioned above]. The values of δ_1 and δ_2 in Si(Li) are thus independent of the deformation.

We also note that the NDE_2 binding energy in the ground state $\{2\Gamma_1^1, \Gamma_4^5; 2\Gamma_6^8\}$ in Si(P) which is strongly compressed along the ⟨100⟩ axis (4.4 ± 0.2 meV) is slightly higher than in undeformed silicon[30] (3.8 ± 0.2 meV). The binding energy of exciton–impurity complexes in Si(Al) falls off from 5.1 meV to 4.2 meV in the deformed crystals, at a valence-band splitting of only $\Delta_{cv} \sim \Delta_{ex} \sim 1$ meV (Ref. 20). This result can be attributed to a decrease in the exchange energy.

7. EFFECT OF A MAGNETIC FIELD IN THE SPECTRA OF MULTIEXCITON–IMPURITY COMPLEXES

a) Zeeman splitting

In the shell model, without the valley-orbit and j–j interactions, the splitting of the emission lines of multiexciton–impurity complexes is determined exclusively by the change in the energy of the recombining pair. In the absence of e-h exchange this change in the energy is the sum of the changes in the energies of the electron and the hole:

$$\hbar\Delta\omega = E_{Hs}^{e} + E_{Hj}^{h}. \tag{32}$$

Unless the field H is very strong, it is sufficient to retain in (32) only the Zeeman splitting, which is linear in the field. The corresponding Hamiltonian for the electrons is[16]

$$\mathscr{H}_H^e = \frac{1}{2}\mu\,[g_\parallel \sigma_z H_z + g_\perp(\sigma_x H_x + \sigma_y H_y)]. \tag{33}$$

The z axis here is along the principal axis of the given extremum. In Eq. (33), μ is the Bohr magneton, σ_i is the Pauli matrix, and g_i are the electron g-factors. According to (33), each electron level of a given valley splits in two, with energies

$$E_{H_s}^{e} = s\mu\sqrt{g_\parallel H_z^2 + g_\perp H_\perp^2}, \quad s = \pm\frac{1}{2}. \tag{34}$$

For silicon, $g_\parallel$ is essentially the same as $g_\perp$, and the splitting does not depend on the direction of **H**:

$$E_{H_s}^{e} = s g_e \mu H. \tag{35}$$

For germanium, with $g_\parallel \neq g_\perp$ the nature of the level splitting is different for the Γ_1 and Γ_5 states. A magnetic field mixes these states. The splitting of the NDE_1 and NDE_2 emission lines with $\Delta_{VO} \neq 0$ is thus not determined by the simple expression in (34). In silicon ($g_\parallel = g_\perp = g_e = 2$) the splitting of the electron levels is the same for all the terms Γ_1, Γ_3, and Γ_5 and is determined by expression (35) even in the case $\Delta_{VO} \neq 0$.

The Hamiltonian describing the Zeeman splitting of the hole levels is

$$\mathscr{H}_H^h = \mu[g_1(\mathbf{JH})^2 + g_2(J_x^3 H_x^3 + J_y^3 H_y^3 + J_z^3 H_z^3)], \tag{36}$$

where g_1 and g_2 are the isotropic and anisotropic hole

TABLE VIII. Relative intensities of the NP lines α_m in a magnetic field in silicon in the Faraday and Voigt arrangements.

j_z	s_z	Faraday geometry		Voigt geometry	
		I_-	I_+	I^π	I^σ
3/2 −3/2	−1/2 1/2	3 −3	3	0	3
1/2 −1/2	1/2 −1/2	1 −1	1	0	1
1/2 −1/2	−1/2 1/2	0 0	0	4	0

g-factors. For free holes, we have $g_2 \ll g_1$, but in the case of bound holes these factors may be comparable in magnitude. At $g_2 = 0$ the four-fold-degenerate Γ_8 state splits into four terms with $j = J_z = \pm 3/2, \pm 1/2$:

$$E_{Hj}^{h} = g_1 \mu H j. \tag{37}$$

For $g_2 \neq 0$ the levels are not spaced uniformly; instead, the spacing depends on the direction of **H** (Ref. 16):

$$E_{H,\pm 3/2}^{h} = \pm 3/2\, g_{h_{3/2}} \mu H, \quad E_{H,\pm 1/2}^{h} = \pm\frac{1}{2} g_{h_{1/2}} \mu H. \tag{38}$$

Under conditions (32), each line in the emission spectra may split into eight parts, corresponding to the two values $s_z = \pm 1/2$ for electrons and the four values of J_z for holes. (In germanium with **H** not along the ⟨100⟩ axis, the splitting $E_{H_s}^{e}$ is different for the different valleys.) The selection rules (Table II) forbid transitions from the (3/2, 1/2) and (−3/2, −1/2) states. In those cases in which the electron and hole spins are parallel, therefore, the corresponding emission lines are not observed. It can be seen from (33) that with $g_\parallel \neq g_\perp$ the spin **s** is not parallel to **H** if **H** is not either parallel or perpendicular to the principal axis. Ac-

TABLE IX. Relative intensities of the TO and TA emission lines in silicon in the Faraday and Voigt arrangements.

j_z	s_z	Faraday geometry		Voigt geometry	
		I_-	I_+	I^π	I^σ
P‖⟨111⟩					
3/2 −3/2	−1/2 1/2	$-9\Phi_T$ $9\Phi_T$	$3(2+\Phi_T)$	$3(1-\Phi_T)$	$\frac{3}{2}(2+\Phi_T)$
1/2 1/2	1/2 1/2	$3\Phi_T$ $3\Phi_T$	$2+\Phi_T$	$1-\Phi_T$	$\frac{1}{2}(2-\Phi_T)$
1/2 −1/2	−1/2 1/2	0 0	$4(1-\Phi_T)$	$2(1+2\Phi_T)$	$2(1-\Phi_T)$
P‖⟨100⟩					
3/2 −3/2	−1/2 1/2	$-6\Phi_T$ $6\Phi_T$	3	3	3/2
1/2 −1/2	1/2 −1/2	$-2\Phi_T$ $2\Phi_T$	1	1	1/2
1/2 −1/2	−1/2 1/2	0 0	4	0	2
$\Phi_T = \frac{\alpha\beta}{\alpha^2+\beta^2}$; $\Phi_T = 0.4$ for $\frac{\alpha}{\beta} = 0.5$.					

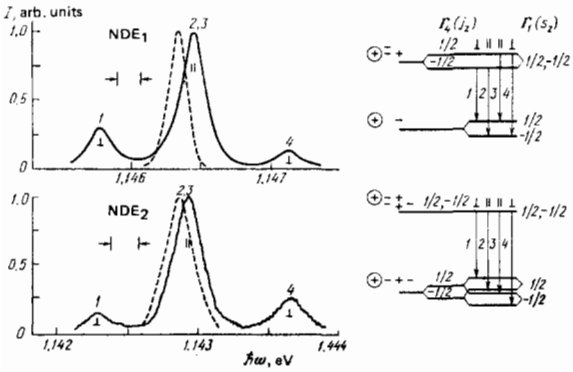

FIG. 19. Splitting of the no-phonon α lines of multiexciton–impurity complexes in compressed Si(P) crystals in a magnetic field.[57] Voigt geometry, $H \perp K$, $H \parallel P \parallel \langle 111 \rangle$, $H = 62$ kOe, $P = 230$ MPa. Dashed curves—Emission lines for $H = 0$; the scheme of allowed transitions is shown at the right.

ground state is not split, the relative intensities of the Zeeman components do not change. The intensity of component 4 in the exciton–impurity complexes decreases with increasing H, in accordance with the interpretation of this component as corresponding to the transition from an excited state. The intensity ratio of the components 4 and 1 in exciton–impurity complexes, however, is an order of magnitude greater than that expected at quasiequilibrium between spin sublevels. The spin-relaxation time in the complexes in deformed Si(P) is thus, at the very least, no shorter than the lifetime of these complexes (10^{-7} s; Ref. 58). Such a pronounced increase in the spin-relaxation time in deformed silicon is attributed to a decrease in the spin–orbit interaction upon lifting of the degeneracy of the valence band.[59]

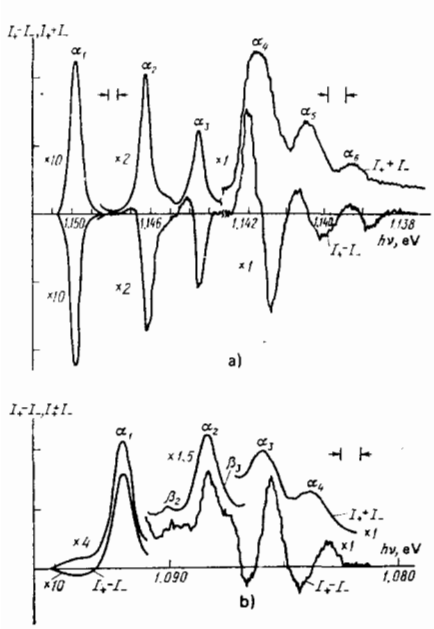

FIG. 20. The emission spectra, $I_+ + I_-$, and the polarizations $I_+ - I_-$. a—Of the no-phonon α lines; b—of the TO components of the α and β lines in the emission spectra of multiexciton–impurity complexes in Si(P) in a magnetic field.[62] $H \parallel \langle 111 \rangle$, $T = 1.9$ K. a) $H = 30$ kOe; b) $H = 50$ kOe.

c) α lines in Si (P) in the Faraday geometry

Figure 20 shows the no-phonon and TO spectra of complexes in undeformed silicon as reported by Altukhov *et al.*[60] They measured both the resultant intensity I_+ and the difference between the intensities of the right-hand and left-hand polarizations, I_-. Since the light is partially depolarized upon reflection from the crystal surfaces, the observed degree of polarization is different from the actual degree. Correspondingly, a correction is made for the depolarization factor in the determination of I_-. The correction is found from the polarization of the no-phonon emission line α_1 of an exciton–impurity complex in a strong magnetic field. In this case, of all the hole levels, only the state with $j_z = -3/2$ is populated, and according to Table VIII the α_1 emission should be completely polarized in the no-phonon line. From Fig. 20 we see that α_1 and α_2 are dinstict emission lines with the polarization σ_-; α_2 is slightly broader than α_1. The $\alpha_3 - \alpha_6$ lines are split into two components, which are clearly observable in the polarized spectrum. These components have different polarizations. For the α_3 lines, the intensity ratio of these components, which is equal to the ratio I_{--}/I_{++}, is 4 : 1, while for the $\alpha_4 - \alpha_6$ lines it is 1 : 1. As mentioned earlier, the shell model predicts that only the state with $j_z = -3/2$ will be populated in an exciton–impurity complex in a strong magnetic field, while in the NDE_2 only the state $J_z = -2$ with $j_z = 3/2$ and $j_z = -1/2$ will be populated. According to Table VIII, the emission is fully polarized (σ_-) for both transitions, $(-3/2, +1/2)$ and $(-1/2, -1/2)$. These two lines are not resolved in the spectrum: All that is seen in some broadening of α_2 in comparison with α_1. In the NDE_3 in a strong field, only the $J_z = -3/2$ term with $j_z = -3/2$, $-1/2$, and $1/2$ is populated in a strong field. In this case the intensity ratio of the right-hand and left-hand polarizations is $I_{++}/I_{--} = 1/4$ (Fig. 20). The lines $\alpha_4 - \alpha_6$ result from the recombination of the Γ_1 electron and holes of the completely filled Γ_8 shell with $J = 0$, so that the intensity ratio for these lines is $I_{++}/I_{--} = 1$. If the α_5 and α_6 lines were a consequence of the recombination of holes of the Γ_x shell, then only the α_5 line or both lines, depending on the degree of degeneracy of this level, would have to be strongly polarized.

The degree of polarization of the α_1 line in the TO spectrum (Fig. 20) is lower than that in the no-phonon spectrum: According to Table VIII with $\Phi_T = 0.4$ we have $P_c = I_{++}/I_{--} = 50\%$ for this line. The polarization in the TO spectrum of the $\alpha_2 - \alpha_4$ lines is even lower, since the unpolarized $(\pm 1/2, \pm 1/2)$ lines are superimposed on the polarized $(\pm 3/2, \pm 1/2)$ and $(\pm 1/2, \pm 1/2)$ lines.

d) Multiexciton–impurity complexes in Si (B) in the Voigt geometry

As mentioned earlier, the j–j splitting is slight in the exciton–impurity complex in Si(B). The paramagnetic splitting of the terms becomes greater than the j–j splitting at $H \geq 30$ kOe. Let us first consider the spectra of complexes in Si(B) which is compressed elastically along the $\langle 111 \rangle$ axis, in which case only the exciton–impurity complexes are stable. The two holes

in an exciton–impurity complex form a singlet state, which is not split. The emission spectrum of the exciton–impurity complex and the transition scheme in this case are qualitatively the same as for an exciton–impurity complex in strongly compressed Si(P) (Ref. 57). The Zeeman components corresponding to the (1/2, – 1/2) and (– 1/2, 1/2) transitions are not resolved, but the line corresponding to these transitions is greatly broadened. The intensity distribution in the Zeeman emission spectrum also implies that a quasiequilibrium is not reached between the spin sublevels during the lifetime of the exciton–impurity complex ($\sim 10^{-6}$ s; Ref. 58), as in compressed Si(P).

In undeformed Si(B), the emission line of an exciton–impurity complex splits into a doublet at $H \sim 60$ kOe (Fig. 21a; Ref. 57). With increasing magnetic field, the intensity ratio of the components (2) and (1) of the m_1 line decreases:

$$\frac{I(2)}{I(1)} \approx 4 \exp\left(-\frac{g_{h_{1/2}}\mu H}{kT}\right).$$

This result means, first, that thermodynamic equilibrium is reached between the spin sublevels for an exciton–impurity complex at boron in undeformed silicon, as for a complex at phosphorus; second, only the component (1) corresponds to a transition from the ground state. In the ground state we thus have $J_z = -2$ and $S_z = -1/2$. Figure 21b shows the scheme of allowed transitions for multiexciton–impurity complexes at boron atoms in silicon in a magnetic field. The energies of the emitted photons are the same for transitions 1 and 3. The coefficient of the exponential function in (39) is related to the difference between the matrix elements for transitions 1 and 2.

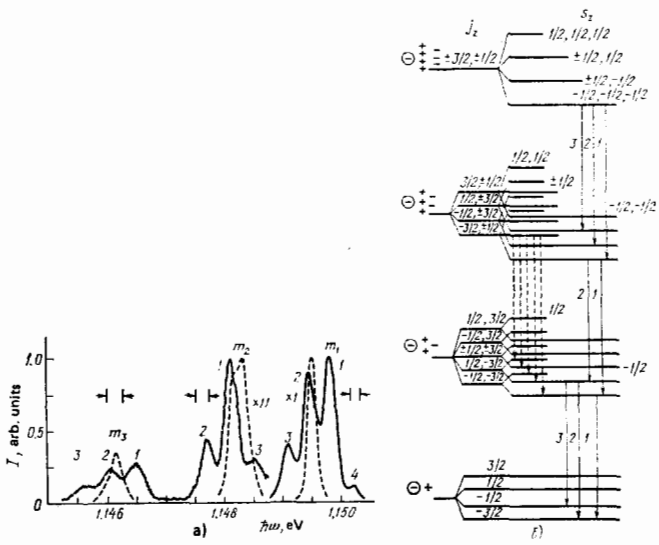

FIG. 21. a—Splitting of the no-phonon lines in the emission spectrum of multiexciton–impurity complexes in Si(B) in a magnetic field[57] [$H = 62$ kOe, $T = 1.8$ K, Voigt geometry ($\mathbf{H} \perp \mathbf{K}$, $\mathbf{H} \parallel \langle 111 \rangle$; dashed curves: Spectrum for $H = 0$; the line α_1(P); emission of NDE_1 at a residual phosphorus impurity]; b—level scheme and allowed transitions of multiexciton–impurity complexes at boron in a magnetic field (the dashed lines are the expected transitions from the ground state of the NAE_2 if two electrons from a spin singlet).

The emission lines of multiexciton–impurity complexes with two and three excitons are split by a strong magnetic field into a doublet and triplet, respectively (Fig. 21). The relative intensities of the Zeeman components in both lines remain the same as the magnetic field is strengthened from 40 to 80 kOe, so that all the components correspond to transitions from the ground state. In order to explain the observed splitting pattern we must assume that the lower-lying state for two electrons in a multiexciton–impurity complex in a magnetic field has a resultant angular momentum projection $S_z = -1$, while that for three electrons has $S_z = -3/2$ (Fig. 21). If two electrons formed a spin singlet Γ_1, the m_2 line would be split into a quintet in a magnetic field, as shown by the dashed lines in Fig. 21b. The measurements in a transverse magnetic field thus agree well with the results found during uniaxial compression.

e) Spectra of complexes of a neutral acceptor with m bound electrons in the case of a strong j-j interaction

The splitting of the NAE_3 emission line in Si(Al) crystals in a magnetic field is precisely the same as that observed in Si(B) (Figs. 21 and 22; Ref. 20). Figure 22b shows the transition scheme in a multiexciton–impurity complex at Al in a magnetic field. In the shell-model study of the level splitting, the slight splitting of the Γ_3, Γ_5 excited state of an exciton–impurity complex corresponding to a total hole angular momentum $J = 2$ is ignored. The ground state of an exciton–impurity complex is a state with $J = 0$ and an electron angular momentum $S_z = -1/2$, as can be seen from the fact that the spectrum of the m_1 line contains three Zeeman components which result from transitions from the lowest-lying state. In transitions from the $J = 2$ state with $s_z = -1/2$, only a single component (–2, –1/2) should be observed. This result agrees with the conclusions reached in a study of the effect of uniaxial deformation (Section 6). Component 4 in Fig. 22 results

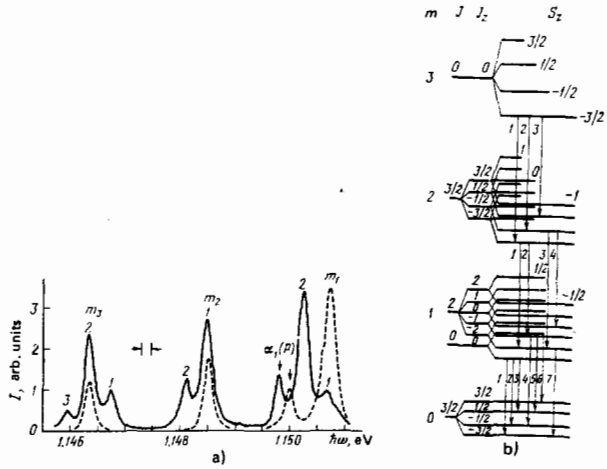

FIG. 22. a—Emission spectrum of multiexciton–impurity complexes in Si(Al) in a magnetic field[20] ($H = 62$ kOe, $\mathbf{H} \perp \mathbf{K}$, $\mathbf{H} \parallel \langle 111 \rangle$, $T = 1.8$ K; the dashed curves show the spectrum for $H = 0$); b—scheme of levels and allowed transitions in multiexciton–impurity complexes in Si(Al) in a magnetic field (the relative arrangement of the levels with $J = 0$ and 2 for the NAE_1 corresponds to $H = 60$ kOe).

in an exciton–impurity complex form a singlet state, which is not split. The emission spectrum of the exciton–impurity complex and the transition scheme in this case are qualitatively the same as for an exciton–impurity complex in strongly compressed Si(P) (Ref. 57). The Zeeman components corresponding to the $(1/2, -1/2)$ and $(-1/2, 1/2)$ transitions are not resolved, but the line corresponding to these transitions is greatly broadened. The intensity distribution in the Zeeman emission spectrum also implies that a quasiequilibrium is not reached between the spin sublevels during the lifetime of the exciton–impurity complex ($\sim 10^{-6}$ s; Ref. 58), as in compressed Si(P).

In undeformed Si(B), the emission line of an exciton–impurity complex splits into a doublet at $H \sim 60$ kOe (Fig. 21a; Ref. 57). With increasing magnetic field, the intensity ratio of the components (2) and (1) of the m_1 line decreases:

$$\frac{I(2)}{I(1)} \approx 4 \exp\left(-\frac{g_{h_{1/2}}\mu H}{kT}\right).$$

This result means, first, that thermodynamic equilibrium is reached between the spin sublevels for an exciton–impurity complex at boron in undeformed silicon, as for a complex at phosphorus; second, only the component (1) corresponds to a transition from the ground state. In the ground state we thus have $J_z = -2$ and $S_z = -1/2$. Figure 21b shows the scheme of allowed transitions for multiexciton–impurity complexes at boron atoms in silicon in a magnetic field. The energies of the emitted photons are the same for transitions 1 and 3. The coefficient of the exponential function in (39) is related to the difference between the matrix elements for transitions 1 and 2.

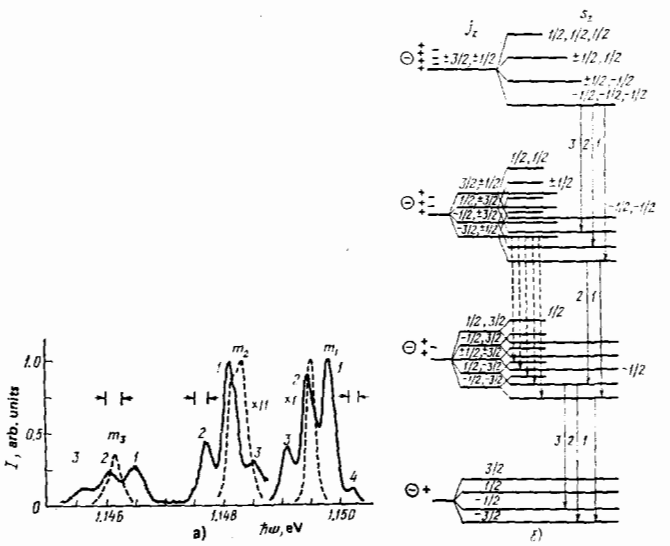

FIG. 21. a—Splitting of the no-phonon lines in the emission spectrum of multiexciton–impurity complexes in Si(B) in a magnetic field[57] [$H = 62$ kOe, $T = 1.8$ K, Voigt geometry ($H \perp K$, $H \parallel \langle 111 \rangle$; dashed curves: Spectrum for $H = 0$; the line α_1(P); emission of NDE_1 at a residual phosphorus impurity]; b—level scheme and allowed transitions of multiexciton–impurity complexes at boron in a magnetic field (the dashed lines are the expected transitions from the ground state of the NAE_2 if two electrons from a spin singlet).

The emission lines of multiexciton–impurity complexes with two and three excitons are split by a strong magnetic field into a doublet and triplet, respectively (Fig. 21). The relative intensities of the Zeeman components in both lines remain the same as the magnetic field is strengthened from 40 to 80 kOe, so that all the components correspond to transitions from the ground state. In order to explain the observed splitting pattern we must assume that the lower-lying state for two electrons in a multiexciton–impurity complex in a magnetic field has a resultant angular momentum projection $S_z = -1$, while that for three electrons has $S_z = -3/2$ (Fig. 21). If two electrons formed a spin singlet Γ_1, the m_2 line would be split into a quintet in a magnetic field, as shown by the dashed lines in Fig. 21b. The measurements in a transverse magnetic field thus agree well with the results found during uniaxial compression.

e) Spectra of complexes of a neutral acceptor with m bound electrons in the case of a strong j-j interaction

The splitting of the NAE_3 emission line in Si(Al) crystals in a magnetic field is precisely the same as that observed in Si(B) (Figs. 21 and 22; Ref. 20). Figure 22b shows the transition scheme in a multiexciton–impurity complex at Al in a magnetic field. In the shell-model study of the level splitting, the slight splitting of the Γ_3, Γ_5 excited state of an exciton–impurity complex corresponding to a total hole angular momentum $J = 2$ is ignored. The ground state of an exciton–impurity complex is a state with $J = 0$ and an electron angular momentum $S_z = -1/2$, as can be seen from the fact that the spectrum of the m_1 line contains three Zeeman components which result from transitions from the lowest-lying state. In transitions from the $J = 2$ state with $s_z = -1/2$, only a single component $(-2, -1/2)$ should be observed. This result agrees with the conclusions reached in a study of the effect of uniaxial deformation (Section 6). Component 4 in Fig. 22 results

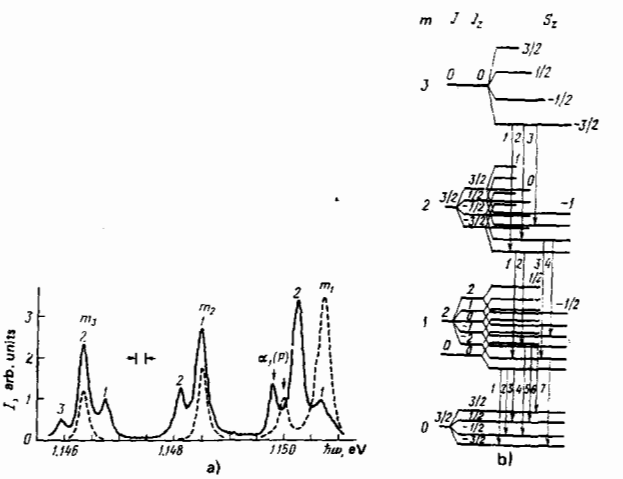

FIG. 22. a—Emission spectrum of multiexciton–impurity complexes in Si(Al) in a magnetic field[20] ($H = 62$ kOe, $H \perp K$, $H \parallel \langle 111 \rangle$, $T = 1.8$ K; the dashed curves show the spectrum for $H = 0$); b—scheme of levels and allowed transitions in multiexciton–impurity complexes in Si(Al) in a magnetic field (the relative arrangement of the levels with $J = 0$ and 2 for the NAE_1 corresponds to $H = 60$ kOe).

from the recombination of an e-h pair in the ($J=0$, $s_z=1/2$) state. Its intensity falls off with increasing magnetic field, but at $H=60-80$ kOe it is an order of magnitude greater than that expected at thermodynamic equilibrium between the $s_z=+1/2$ and $-1/2$ sublevels. The components corresponding to transitions 5 and 6 cannot be resolved; they overlap lines 1 and 2, because g_e is approximately equal to the sum $g_{h_{1/2}}+g_{h_{3/2}}$ at a neutral acceptor. At 2 K, the spectrum does not reveal the components corresponding to the recombination of e-h pairs in an exciton–impurity complex in the $(-2,-1/2)$ state, which lies below $\{1;1/2\}$ but above $\{0,-1/2\}$ at $H=40$ kOe (Ref. 20). In the exciton–impurity complex, therefore, there is a deviation from equilibrium only between the electron states of the $J=0$ term. This is not a surprising result, since with $J=0$ the electron–hole exchange interaction— the most efficient spin-relaxation channel— is greatly suppressed. Equilibrium is attained between the states with $J=2$ and $J=0$ at $H\neq 0$, as at $H=0$.

In NAE_2 transitions from the $(-3/2,-1)$ ground state are forbidden in exciton–impurity complexes with $J=0$. In strong fields ($H\gtrsim 50$ kOe), therefore, the emission spectrum of NAE_2 contains only two lines, corresponding to transition to the $J=2$ states with $J_z=-2$ and $J_z=-1$, as in Si(B). At this point it is not clear, however, why the intensity of the line corresponding to the transition from the $(-1/2;-1)$ excited state is higher in Si(Al) than in Si(B). In Si(Al) this line can be seen well even at $H\sim 60$ kOe (Fig. 22; Ref. 20).

f) Polarization of the emission of multiexciton–impurity complexes in a longitudinal magnetic field

The individual Zeeman components cannot be resolved in weak fields, especially in a study of the phonon lines in the spectra of multiexciton–impurity complexes. An effective approach in such cases is to measure the degree of polarization of all the lines together. This method has revealed, in particular, a difference between the spectra of multiexciton–impurity complexes with different numbers of excitons,[61] despite the superficial similarity of the Zeeman distributions observed in Ref. 7.

As mentioned earlier, the polarization of each of the Zeeman components in a multiexciton–impurity complex does not depend on the number of excitons and is determined instead by the values of $I_\pm(j_z,s_z)$ in Tables VIII and IX.

The relative intensities W of these components depend on the populations of the corresponding states, i.e., on the number of bound excitons (m), the nature of the filled shell $r(\Gamma_1,\Gamma_{3,5})$ and the temperature. These intensities $W_m^r(s_z,j_z)$ are given by[61]

$$W_m^r(s_z,j_z)=\sum_{S_z} g^r_{S_z,m}\nu^{S_z,r}_{s_z,m}\exp\left(-\frac{g_e\mu HS_z}{kT}\right)\sum_{J_z}\nu^{J_z}_{j_z,m}\exp\left(-\frac{g_h\mu HJ_z}{kT}\right). \tag{40}$$

Here $g^r_{S_z,m}$ is the statistical weight of the state with the total electron angular momentum S_z, i.e., the number of combinations with which the state with the given value of S_z can exist in the shell r of a complex with m electrons. The number $\nu^{S_z,r}_{s_z,m}$ is the number of electrons with spin s_z in shell r in the state S_z for a given number $(m-1)$ of electrons for the $\Gamma_{3,5}$ shell in NDE_m and for the number m for the $\Gamma_{1,3,5}$ shell in NAE_m. Finally, $\nu^{J_z}_{j_z,m}$ is the number of holes with angular momentum j_z in the state with total angular momentum J_z for a given number of holes (m) in NDE_m and $m+1$ in NAE_m.

According to the Pauli principle, $\nu^{J_z}_{j_z,m}$ takes on the values 0 and 1, except for exciton–impurity complexes at acceptors, in which we have $\nu^0_{j_z,1}=1/2$ for all four values $j_z=\pm 3/2,\pm 1/2$ for the terms $J=0$ with $J_z=0,2$. In complexes at neutral donors for the term Γ_1 with $S=0$ we have $\nu^{0,\Gamma_1}_{s_z,m}=1$ for all $s_z=\pm 1/2$ and for all m, so that $W_m^{\Gamma_1}(s_z,j_z)$ does not depend on s_z for the α lines:

$$W_m^{\Gamma_1}(s_z,j_z)=\sum_{J_z}\nu^{J_z}_{j_z,m}\exp\left(-\frac{g_{h_{j_z}}\mu H_{j_z}}{kT}\right). \tag{41}$$

The degree of circular polarization of the emission in the X_m^r lines is

$$P_c(X_m^r)=\sum_{s_z,j_z} I_-(s_z,j_z)W_m^r(s_z,j_z)\Big[\sum_{s_z,j_z} I_+(s_z,j_z)W_m^r(s_z,j_z)\Big]^{-1}, \tag{42}$$

where $X_m^{\Gamma_1}=\alpha_m$, $X_m^{\Gamma_{3,5}}=\beta_{m-1}$ for NDE_m and $X_m^{\Gamma_{1,3,5}}=m_m$.

The polarization of the emission lines of Si(P) and Si(B) in a longitudinal magnetic field was studied in Refs. 60–62.

Figure 23 shows the dependence $P_c(H)$ for the α_m (NP and TO) and β_{m-1}(TO) emission lines of complexes with $m=1-6$ in Si(P). The degree of polarization of the α lines falls off with increasing number of bound excitons; the NP and TO lines have different polarization, because of the difference in the signs of I_- (Tables VIII and IX). The $\alpha_4-\alpha_6$ lines are unpolarized, since they are a consequence of the recombination of holes and electrons from the filled Γ_8 and Γ_1 shells. The polarization of the β_1 and β_2 lines is also determined primarily by the orientation of the holes, and it has the same sign as the polarization of the TO lines α_2 and α_3. The polarization has the opposite sign for the β_3 line, since the holes are unpolarized in a complex with $m=4$, and the orientation of the electrons leads to a polarization of the opposite sign, as can be seen from Tables VIII and IX. Figure 24 shows the dependence

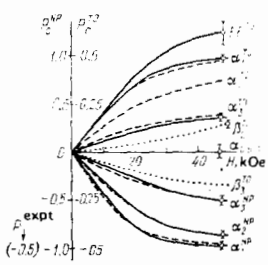

FIG. 23. Circular polarization of the no-phonon (NP) and transverse optical (TO) components of the emission line of multiexciton–impurity complexes in Si(P) ($\alpha_m^{NP\,TO}$ and β_m^{TO}) and of a free exciton (FE) in a magnetic field in the Faraday configuration.[62] H ∥ ⟨111⟩, $T=1.9$ K. Solid curves—Experimental; circles and dashed curves—theoretical for $g_e=2$, $g_h=1.2$ and $T=1.9$ K.

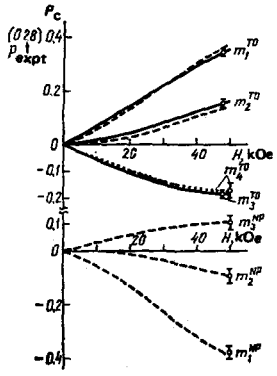

FIG. 24. Circular polarization of the NP and TO emission lines of multiexciton–impurity complexes in Si(B) in a magnetic field.[63] H ∥ ⟨111⟩, $T = 1.9$ K, $N_B = 3 \cdot 10^{15}$ cm^{-3}. Solid curves—Experimental; dashed curves—theoretical for $g_e = 2$ and $g_h = 1.2$.

$P_c(H)$ for the NP and TO lines of NAE_m with $m = 1$–4. The sign of the polarization of the m_1 and m_2 lines is determined by the orientation of the holes, while that of the m_3 and m_4 lines (which result from the recombination of holes from the $J = 0$ state) is determined by the orientation of the electrons. They accordingly have different polarization signs. The theoretical curves in Fig. 24 were plotted from Eqs. (40)–(42) for the values $\alpha/\beta = 0.5$, $g_1 = 1$, 2, $g_e = 2$.

According to Altukhov *et al.*,[63] the agreement between theory and experiment can be improved by assuming that there is a slight valley–orbit splitting of the opposite sign in the complexes at neutral acceptors, i.e., by assuming that the $\Gamma_{3,5}$ electron levels are the lower levels in these complexes, as in complexes at lithium neutral donors. Under this assumption, the splitting Δ_{mVO} should increase slightly with increasing m, from 0.05 meV at $m = 1$ to 0.16 meV at $m = 3$. The valley–orbit splitting is not observed directly in the NAE_m spectra.

Figure 23 also shows the $P_c(H)$ dependence for the TO line of a free exciton (FE). There is some difference between the values of P_c at saturation for the free exciton and the exciton–impurity complex, which is possibly a consequence of the difference between the selection rules for free and bound excitons, mentioned earlier. The curves in Fig. 24 were recorded with H ∥ ⟨111⟩. It can be seen from Table IX that the degree of polarization of the TO lines depends on the direction of the magnetic field: If H is not directed along the ⟨111⟩ or ⟨100⟩ principal axis, a linear polarization should also arise in a longitudinal field.[64] With H ∥ ⟨110⟩, for example, the intensities of the TO lines in the e ∥ ⟨001⟩ and e ∥ ⟨110⟩ polarizations are different. According to the calculations of Ref. 64, the degree of linear polarization $P_1 = (I_{001} - I_{1\bar{1}0})/(I_{001} + I_{1\bar{1}0})$ reaches 31% and 11% for the TO lines α_1 and α_3, respectively. The α_2 and α_4 lines are not linearly polarized. These calculations correspond to $g_2 = 0$. The anisotropy of the g-factor of the holes should also lead to a polarization of the α_m no-phonon lines. With $g_1 = 0.6$ and $g_2 = 0.4$ for the α_1 line we thus have $P_1 = 10\%$; for α_3 we have $P_1 = 6\%$; and the α_2 and α_4 lines are unpolarized. The appearance of a linear polarization in the Faraday geometry with H ∥ ⟨110⟩ has been observed at bound excitons in Ga(As) (Ref. 65). This phenomenon has not been studied in detail experimentally.

TABLE X. The g-factors of bound electrons and holes in multiexciton–impurity complexes, neutral donors and neutral acceptors and parameters characterizing the diamagnetic shift in multiexciton–impurity complexes in silicon (H ∥ ⟨111⟩), according to the data of Refs. 12, 57, 66, 67, and 68.

	NDE_1 Si (As)[12]	NDE_1 Si (P)[66]	NDE_2–NDE_4 Si (P)[57]	ND Si (P)[67]	NA Si (B)[68]	NAE Si (B)[57]
g_e	1.85	1.99	2.0	2.0	—	1.85
$g_{h1/2}$	1.46	1.54	1.8	—	1.15	1.2
$g_{h3/2}$	1.17	1.27	1.2	—	1.1	1.1
g_1	0.74	0.86	0.6	—	1.03	1.2
g_2	0.22	0.21	0.4	—	0.04	0.1
$b_{1/2} \cdot 10^5 \frac{\text{meV}}{\text{kOe}^2}$	1.85 *)	1.5	2.2 *)	—	—	2 *)
$b_{3/2} \cdot 10^5 \frac{\text{meV}}{\text{kOe}^2}$		3.4				

*)Average value.

g) The g-factors of electrons and holes in multiexciton–impurity complexes

From the splitting of the emission lines of multiexciton–impurity complexes we can determine the g-factors of the recombining electrons and holes. The results[13,57,66] are shown in Table X, along with the g-factors of an electron in a neutral donor and of a hole in a neutral acceptor.[67,68] It can be seen from this table that the g-factors of electrons in multiexciton–impurity complexes at donors and acceptors essentially agree with the g-factor of an electron in a neutral donor, within the experimental errors. The g-factors of the holes, on the other hand, agree with the g-factor of the holes in the boron neutral acceptor only in a multiexciton–impurity complex at a boron atom; they are quite different from g_h in Si(B) in multiexciton–impurity complexes at donors. The splitting of the hole levels in the magnetic field is determined by Hamiltonian (36). With $g_2 \neq 0$ the magnitude of the splitting depends on the direction of the magnetic field, and the g-factors of the holes, $g_{h_{3/2}}$ and $g_{h_{1/2}}$ are not the same. With H ∥ ⟨111⟩, for example, we have[16]

$$g_{h_{1/2}} = g_1 + \frac{13}{4} g_2, \quad g_{h_{3/2}} = \frac{1}{3} \sqrt{6 \left(g_1 + \frac{9}{4} g_2\right)^2 + 3 \left(g_1 + \frac{5}{4} g_2\right)^2}. \quad (43)$$

In deformed silicon with H ∥ P ∥ ⟨111⟩ we have[16]

$$g_{h\parallel} = g_1 + \frac{13}{4} g_2. \quad (44)$$

From Table X we see that in a multiexciton–impurity complex at phosphorus the difference $g_{h_{3/2}} - g_{h_{1/2}}$ is much larger than in a neutral acceptor. The difference between the values of the constant g_2 for free and bound excitons is a consequence of the smooth functions of the $d, g, \ldots$ types for the holes bound at the center or in the exciton.[16] The large values of g_2 in complexes at neutral donors indicate a large amplitude for the $d, g, \ldots$ functions. This is a natural difference, since it is not energetically favorable for holes in multiexciton–im-

purity complexes at neutral donors to be positioned near the positively charged donor. Consequently, the contribution of the $d, g, \ldots$ functions, which vanish at the donor, increases. Finally, we note that the difference between $g_{h_{3/2}}$ and $g_{h_{1/2}}$ was ignored in the plotting of the theoretical curves $P_c(H)$ in Fig. 23, and it was assumed that $g_h = 1, 2$. The reason for this approach is that the contribution from the hole with $j_z = 3/2$ is predominant for the α_m lines in strong magnetic fields. The replacement of g_h by $g_{h_{3/2}} = 1, 2$ thus leads to good agreement with the theory, even at significant values of g_2.

h) Diamagnetic splitting of the terms of exciton–impurity complexes at neutral donors in germanium

In strong magnetic fields, the emission spectra of free and bound excitons should exhibit, along with the Zeeman splitting, a diamagnetic splitting which is quadratic in the field and also a diamagnetic level shift. These effects are most pronounced in germanium, where the exciton radius is much larger than in silicon. The diamagnetic splitting of the electron levels results from a difference between the longitudinal and transverse effective electron masses, $m_\parallel$ and $m_\perp$. With H not along the ⟨100⟩ axis in germanium, the states corresponding to different valleys undergo different shifts. The shift is given by

$$\Delta_{e\,\mathrm{dia}}^{l} = \lambda_2 H^2 (3\cos^2\theta_l - 1), \tag{45}$$

where θ_l is the angle between H and the principal axis of the valley, z_l. Under the condition $m_\parallel > m_\perp$, which holds in germanium and silicon, we have $\lambda_2 > 0$. In excitons bound to neutral donors in germanium, the diamagnetic shift in (45) leads to a splitting of the Γ_5 terms and to their mixing with Γ_1 terms. In a strong magnetic field, in which the diamagnetic splitting is greater than the valley–orbit splitting, the low-lying levels in the case H ∥ ⟨111⟩ correspond to the valleys $(11\bar{1})$, $(1\bar{1}1)$, and $(\bar{1}11)$. These three states are split by the spin–orbit interaction into two terms, Γ_1 and Γ_3. With H ∥ ⟨110⟩, the low-lying levels correspond to $(1\bar{1}1)$ and $(\bar{1}11)$ valleys. Like the two upper states, these two states are split by the valley–orbit interaction. Diamagnetic effects also split the ± 3/2 and ± 1/2 hole terms. This splitting is described by a Hamiltonian similar to the deformation Hamiltonian.[16] In the spherical approximation, it is given by

$$H_{h\,\mathrm{dia}} = \bar{\lambda}_3 \left[(\mathbf{JH})^2 - \frac{5}{4} H^2 \right]. \tag{46}$$

In germanium, $\bar{\lambda}_3 > 0$. Because of diamagnetic effects and the anisotropy of the hole g-factor, the nature of the splitting of the levels of an exciton–impurity complex and the polarization of the LA lines depend on the direction of the magnetic field. Since the diamagnetic splitting of the Γ_5 term for an exciton bound to a neutral donor, given by (45), may be comparable to or even greater than the valley–orbit splitting, the change in the polarization in a longitudinal magnetic field and also the level splitting are quite different in the cases H ∥ ⟨100⟩, ⟨111⟩, and ⟨110⟩. The situation is shown clearly by Fig. 25, which shows the dependence $P_c(H)$ for the no-phonon lines of exciton–impurity complexes

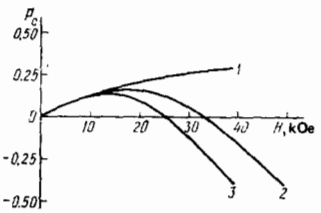

FIG. 25. Circular polarization of the NP lines of NDE in Ge(As) in a magnetic field.[65] $T = 1.9$ K, $N_{As} = 2 \cdot 10^{15}$ cm^{-3}. 1—H ∥ ⟨100⟩; 2—H ∥ ⟨110⟩; 3—H ∥ ⟨111⟩.

in Ga(As) for these three directions of the magnetic field.[65]

i) Diamagnetic shifts of the lines of multiexciton–impurity complexes in silicon

In fields $H > 30$ kOe, the emission lines of multiexciton–impurity complexes in silicon exhibit a shift which is quadratic in the field.[57] This shift can be seen particularly well for the narrow emission line of an exciton–impurity complex in Si(P). The behavior of the emission line of an exciton–impurity complex in Si(P) was recently studied in detail by Kaminskiĭ *et al.*[6] at $T = 4.2$ K, at which the population of the excited spin states is quite high up to $H \sim 60$ kOe. Analyzing the quadratic shifts of all six Zeeman components, Kaminskiĭ *et al.* also distinguished a contribution from the diamagnetic splitting of the ± 3/2 and ± 1/2 hole terms. This splitting turned out to be very large at H ∥ ⟨111⟩ (Table X).

A determination of the diamagnetic properties is of particular interest because of the possibility of evaluating the size of a complex. For spherically symmetric wave functions, the diamagnetic shift Δ_{dia} is related in first-order perturbation theory to the average particle radius in the complex by the Langevin relation[69]

$$\Delta_{\mathrm{dia}} = \frac{e^2 H^2}{12c^2} \sum_i \frac{\langle r_i^2 \rangle}{m_i}, \tag{47}$$

where the sum is over both the electron and hole states.

If we assume that the relation $\langle r_i^2 \rangle = 3a_B^2$ holds in the complex (as for the 1s hydrogen-like wave function) and also that the radii of the electron and hole shells are equal, by virtue of the approximately equal effective masses of the electrons and holes, then we find the value[57] $r_i \approx 0.65$, $a_{B,\,\mathrm{FE}} \approx 30$ Å for the radius of an exciton–impurity complex in Si(P) and Si(B). The radius of an exciton–impurity complex is thus smaller than the exciton radius, in accordance with calculations in Ref. 70. We will point out, however, that the value found for r_i for an exciton–impurity complex through the use of the Langevin equation, without the Van Vleck term, of paramagnetic origin, which arises in second-order perturbation theory and which has the opposite sign, may turn out to be somewhat too low.

Analysis of the diamagnetic shifts of the emission lines of multiexciton–impurity complexes in Si(B) for transitions between ground states with the help of expression (47) from Ref. 57 revealed that the size of the complexes remains essentially constant as the number of e-h pairs

bound to the center increases. It follows that the electron–hole density increases with increasing number of e-h pairs in the complex. This conclusion agrees with calculations in Ref. 70. The "self-compression" of complexes with increasing number of e-h pairs observed in research on diamagnetic shifts also correlates well with the decrease in the radiationless lifetime of e-h pairs in these complexes. In indirect semiconductors this time is known to be determined primarily by radiationless Auger recombination.

8. ELECTRON–HOLE AND ELECTRON–ELECTRON EXCHANGE AND FINE STRUCTURE OF THE LEVELS OF MULTIEXCITON–IMPURITY COMPLEXES IN SILICON

The fine structure of the α emission line of NDE_2 in silicon was recently resolved for the first time.[26,71] Kaminskiĭ *et al.*[71] used silicon samples grown by crucible-free zone crystallization and doped with phosphorus through neutron bombardment. In those samples the width of the α line of NDE_1, which has no fine structure, was less than 5 μeV. A high resolution was achieved through the use of a Fabry–Perot interferometer. It was found that the α_2 line, corresponding to the $\{2\Gamma_1, \Gamma_{3,5}, 2\Gamma_8\} - \{\Gamma_1, \Gamma_{3,5}, \Gamma_8\}$ transition, consists of a large number of components, related to the splitting of both the initial and final states. Particularly interesting was the detection of a fine structure of the α_2 line in samples compressed along the ⟨001⟩ axis, in which case three components were reliably resolved in the spectrum.[71] In the deformed crystal the initial state of the NDE_2 is degenerate only in the spin of the Γ_4 electron and is not split. The spins of the two other Γ_1 electrons, and also the spins of the two Γ_6 holes, are antiparallel. In the final state, NDE_1^*, there are two electrons, Γ_1 and Γ_4, and a Γ_6 hole, and the sole reason for the splitting of this excited state is the exchange interaction. These experiments thus yielded the first direct determination of the magnitude of the exchange splitting in silicon. Kaminskiĭ *et al.*[71] considered the exchange only between the Γ_4 electron and the Γ_6 hole. This model explains the observed splitting of the α_2 line, but it fails to explain the intensity ratios of the components. As mentioned earlier, the shell model predicts that the smooth wave functions of the Γ_4 and Γ_1 states will be the same, so that the e-h exchange for the Γ_1 and Γ_4 electrons should also be the same, described by

$$\mathscr{H}_{eh}^{ex} = \Delta_\perp (JS) + (\Delta_\parallel - \Delta_\perp) J_z S_z, \tag{48}$$

where J is the angular momentum of the Γ_6 hole ($J_z = \pm 1/2$), and $S = s_1 + s_4$ is the resultant angular momentum of the Γ_1 and Γ_4 electrons ($S = 0; 1$). In addition to the e-h exchange it is necessary to consider the e-e exchange between the electrons of different valleys. In silicon, this latter exchange is essentially isotropic. It leads to an exchange interaction of Γ_1 and Γ_4 electrons given by

$$\mathscr{H}_{ee}^{ex} = \Delta_3 (S_1 S_4) = \frac{1}{2} \Delta_3 \left(S^2 - \frac{3}{2} \right). \tag{49}$$

The constants $\Delta_\perp$, $\Delta_\parallel$, and Δ_3 should be nearly equal in order of magnitude, since the e-e exchange, like the e-h exchange, is determined by a short-range interaction.[16,72] According to (48) and (49) the α_2 line in a crystal compressed along the ⟨001⟩ axis should consist of four components, with positions and intensities in the $\pi(I_\parallel)$ and $\sigma(I_\perp)$ polarization determined by Table XI (Ref. 72). This model yields a satisfactory explanation for both the positions and relative intensities of the lines observed by Kaminskiĭ *et al.*[71] if we set $\Delta_3 = 104$ μeV, $\Delta_\perp = -47$ μeV, and $\Delta_\parallel = -12$ μeV (Ref. 72).

TABLE XI. Relative positions of E and of the intensity in the π ($I_\parallel$) and σ ($I_\perp$) polarizations of the components of the α_2 line in silicon compressed along the ⟨001⟩ axis ($R = \sqrt{1+8\xi^2}$, where $\xi = \Delta_\perp/\Delta_\parallel$).

N	E	Intensity	
		$I_\parallel$	$I_\perp$
I	Δ_{ee}^{ex}	2	1/2
II	$\Delta_\parallel (R-1)/4$	$3 - R^{-1}(1+8\xi)$	$(1+R^{-1})/4$
III	$2\Delta_\parallel/4$	0	1
IV	$-\Delta_\parallel (R+1)/4$	$3 + R^{-1}(1+8\xi)$	$(1-R^{-1})/4$

In the undeformed crystal the e-h crystal is determined by the expression[16]

$$\mathscr{H}_{eh}^{ex} = 2\Delta_1 (JS) + 2\Delta_2 \sum_i J_i S_i. \tag{50}$$

At a small deformation, such that the deformation splitting of the Γ_8 level is small in comparison with the binding energy, the constants $\Delta_\perp$ and $\Delta_\parallel$ in (48) are related to Δ_1 and Δ_2 in (50) by $\Delta_\perp = 4\Delta_1 + 10\Delta_2$, $\Delta_\parallel = 2\Delta_1 + 1/2\Delta_2$ (for compression along the ⟨001⟩ axis) or $\Delta_\perp = 3\Delta_2$, $\Delta_\parallel = 6\Delta_1 + 27/2\Delta_2$ (for extension along ⟨001⟩). These values of $\Delta_\parallel$ and $\Delta_\perp$ corresponds to $\Delta_1 = -48$ μeV and $\Delta_2 = -17$ μeV, in agreement with the estimates $|\Delta_{eh}^{ex}| \approx 50$ μeV made in Ref. 73 on the basis of the spin-relaxation time of the electron in the exciton. In the undeformed crystal, the structure of the lower term of NDE_2, $\{2\Gamma_1, \Gamma_5, \Gamma_8\}$, is determined by the j–j splitting and the crystal splitting (discussed in Section 4) in addition to e-h exchange, while the structure of the NDE_1^* term $\{\Gamma_1, \Gamma_5, \Gamma_8\}$ is determined by e-e exchange, e-h exchange, and the crystal splitting. The exchange–valley interaction leads only to an identical shift of all the sublevels of this state. The magnitudes of these splittings cannot be determined unambiguously from the data of Ref. 71. This determination could apparently be made if measurements were carried out at lower temperatures, so that the population of the upper states of the NDE_2 could be changed.

9. CONCLUSION

We have focused primarily on multiexciton complexes in silicon in this review, because the corresponding research has been most thorough in this semiconductor. It is apparently in silicon that the properties of multiexciton–impurity complexes can be described best by the one-electron theory on which the shell model is based. As mentioned above, multiexciton–impurity complexes are observed in Ge, GaP, and SiC as well as Si. The formation of such complexes at shallow im-

purity centers is a common phenomenon and can be expected in other semiconductors with degenerate bands. In direct-gap semiconductors with the sphalerite structure, where the extremum of the upper valence band is fourfold degenerate in the spin, there may be a stable complex NAE_2 in addition to bound excitons at neutral donors and neutral acceptors. Although the shell model furnishes a qualitative and frequently quantitative description of the properties of multi-exciton–impurity complexes in silicon, there are many other questions regarding the internal structure of the multiexciton–impurity complexes which remain unanswered. For example, we do not yet know how the upper (excited) hole shells of the complex are filled and just how stable the complexes are under these conditions. In this connection it would be interesting to see just how many e-h pairs can be bound to a center and form a stable complex. A theoretical study of this question would be interesting. The one-electron approach, which is presently being used to describe the energy spectrum and the filling of the shells of multiexciton–impurity complexes, is only a crude approximation. It is thus natural to expect to find a fine structure in the spectrum due to electron–electron (or electron–hole) correlations. Experiments on germanium and silicon confirm these expectations, but as yet there has been no detailed study of the observed fine structure, and the particular mechanisms responsible for the observed level splitting have not been determined. The electron–electron collective interactions should also lead to a change in the g-factors of the electrons. It would therefore be interesting to see precise measurements of the paramagnetic splitting in multiexciton–impurity complexes with different number of bound excitons.

The multiexciton–impurity complexes at neutral impurities contain an odd number of particles (electrons or holes), so that these complexes should be paramagnetic centers. Consequently, a study of the electron-spin-resonance spectra of such complexes and the development of optical methods for detecting the ESR spectra might prove sensitive methods for studying the internal structure of these complexes.

We will conclude by pointing out that the many-particle exciton–impurity complex in a semiconductor is not amenable to a rigorous theoretical description, because the problem lacks a small parameter. There is accordingly definite interest in variational calculations of the ground-state energy of multiexciton–impurity complexes; the results could be used to analyze the stability of the multiexciton–impurity complexes upon a change in the number of bound excitons.

[1]M. A. Lampert, Phys. Rev. Lett. 1, 450 (1958).
[2]J. R. Haynes, Phys. Rev. Lett. 4, 361 (1960).
[3]A. S. Kaminskiĭ and Ya. E. Pokrovskiĭ, Pis'ma Zh. Eksp. Teor. Fiz. **11**, 381 (1970). [JETP Lett. **11**, 255 (1970)].
[4]A. S. Kaminskiĭ, Ya. E. Pokrovskiĭ, and N. V. Alkeev, Zh. Eksp. Teor. Fiz. 59, 1937 (1970) [Sov. Phys. JETP 32, 1048 (1971)].
[5]Ya. E. Pokrovskiĭ, A. S. Kaminskiĭ, and K. Svistunova, in: Proc. of Tenth Intern. Conference on Physics of Semiconductors, Cambridge, 1970, p. 504.
[6]R. Sauer, Phys. Rev. Lett. **31**, 376 (1973).
[7]K. Kosai and M. Gershenzon, Phys. Rev. B9, 723 (1974).
[8]R. Sauer and J. Weber, Phys. Rev. Lett. **36**, 48 (1976).
[9]R. Sauer, W. Schmid, and J. Weber, Solid State Commun. **24**, 507 (1977).
[10]J. S. -Y. Wang and C. Kittel. Phys. Lett. **A42**, 189 (1972).
[11]D. G. Thomas, M. Gershenzon, and J. J. Hopfield, Phys. Rev. **131**, 2397 (1963).
[12]J. M. Cherlow, R. L. Aggarwal, and B. Lax, Phys. Rev. **B7**, 4547 (1973).
[13]P. J. Dean, D. C. Herbert, D. Bimberg, and W. J. Choyke, Phys. Rev. Lett. **37**, 1635 (1976).
[14]G. Kirczenow, Solid State Commun. **21**, 713 (1977).
[15]G. Kirczenow, Can. J. Phys. **55**, 1787 (1977).
[16]G. L. Bir and G. E. Pikus, Simmetriya i deformatsionnye éffekty v poluprovodnikakh (Symmetry and Deformation Effects in Semiconductors), Nauka, Moscow, 1972.
[17]N. O. Lipari and A. Baldereschi, Solid State Commun. **25**, 665 (1978).
[18]M. L. W. Thewalt, Can. J. Phys. **55**, 1463 (1977).
[19]V. D. Kulakovskiĭ, in: Tezisy Vsesoyuznogo soveshchaniya po fizike éksitonov (Abstracts, All-Union Conference on the Physics of Excitons), Leningrad, 1977, p. 28; Pis'ma Zh. Eksp. Teor. Fiz. **27**, 217 (1978) [JETP Lett. **27**, 202 (1978)].
[20]V. D. Kulakovskii and A. V. Malyavkin, Phys. Status Solidi **B92**, 455 (1979).
[21]S. A. Lyon, D. L. Smith, and T. C. McGill, Phys. Rev. **B17**, 2620 (1978).
[22]K. R. Elliott, B. S. Osbourn, D. L. Smith, and T. C. McGill, Phys. Rev. B17, 1808 (1978).
[23]M. L. W. Thewalt, Phys. Rev. Lett. **38**, 521 (1977).
[24]E. C. Lightowlers and M. O. Henry, J. Phys. C 10, L247 (1977).
[25]G. E. Pikus, Fiz. Tverd. Tela (Leningrad) 19, 1653 (1977) [Sov. Phys. Solid State **19**, 965 (1977)].
[26]R. R. Parsons, Solid State Commun. 22, 671 (1977).
[27]A. E. Mayer and E. G. Lightowlers, J. Phys. C **12**, L539, L945 (1978).
[28]S. A. Lyon, D. L. Smith, and T. C. McGill, Phys. Rev. Lett. **41**, 56 (1978).
[29]S. A. Lyon, D. L. Smith, and T. C. McGill, Solid State Commun. 28, 317 (1978).
[30]M. L. W. Thewalt, J. A. Rostworowski, and G. Kirczenow, Can. J. Phys. **57**, 1898 (1979).
[31]P. J. Dean, J. R. Haynes, and W. F. Flood, Phys. Rev. **161**, 711 (1967).
[32]T. Nishino, H. Nakayama, and Y. Hamakawa, Solid State Commun. **21**, 327 (1977).
[33]M. O. Henry and E. C. Lightowlers, J. Phys. C **10**, L601 (1977).
[34]A. S. Kaminskiĭ and Ya. E. Pokrovskiĭ, Zh. Eksp. Teor. Fiz. 75, 1037 (1978) [Sov. Phys. JETP **48**, 523 (1978)].
[35]R. W. Martin, Solid State Commun. **14**, 369 (1974).
[36]G. E. Pikus and N. S. Averkiev, Pis'ma Zh. Eksp. Teor. Fiz. **32**, 352 (1980) [JETP Lett. **32**, 328 (1980)].
[37]M. Taniguchi, M. Hirano, and S. Narita, Phys. Rev. Lett. **35**, 1095 (1975).
[38]M. Taniguchi and S. Narita, J. Phys. Soc. Jpn **43**, 1262 (1977).
[39]E. O. Kane, Phys. Rev. **B11**, 3850 (1975).
[40]G. A. Thomas, A. Frova, J. C. Hensel, R. E. Miller, and P. A. Lee, Phys. Rev. **B13**, 1692 (1976).
[41]R. B. Hammond, D. L. Smith, and T. C. McGill, Phys. Rev. Lett. **35**, 1535 (1975).
[42]V. M. Asnin, G. L. Bir, Yu. N. Lomasov, G. E. Pikus, and A. A. Rogachev, Zh. Eksp. Teor. Fiz. 71, 1600 (1976) [Sov. Phys. JETP **44**, 838 (1976)].
[43]M. Lax and J. J. Hopfield, Phys. Rev. **124**, 115 (1961).
[44]P. D. Altukhov, G. E. Pikus, and A. A. Rogachev, Fiz. Tverd. Tela (Leningrad) 20, 489 (1978) [Sov. Phys. Solid

State 20, 283 (1978)].
[45]N. V. Alkeev, A. S. Kaminskiĭ, and Ya. E. Pokrovskiĭ, Fiz. Tverd. Tela (Leningrad) 17, 843 (1975) [Sov. Phys. Solid State 17, 535 (1975)].
[46]I. Balslev, Phys. Rev. 141, 636 (1966).
[47]R. Sauer and J. Weber, Phys. Rev. Lett. 39, 770 (1977).
[48]A. S. Kaminskiĭ, V. A. Karasyuk, and N. E. Pokrovskiĭ, Zh. Eksp. Teor. Fiz. 74, 2234 (1978) [Sov. Phys. JETP 47, 1162 (1978)].
[49]V. D. Kulakovskiĭ, Fiz. Tverd. Tela (Leningrad) 20, 1394 (1978) [Sov. Phys. Solid State 20, 802 (1978)].
[50]G. L. Bir and G. E. Pikus, Fiz. Tverd. Tela (Leningrad) 17, 696, 1284 (1975) [Sov. Phys. Solid State 17, 448, 830 (1975)].
[51]E. Karteuser and S. Rodriguez, Phys. Rev. B8, 1556 (1973).
[52]H. R. Chandrasekhar, P. Fisher, A. K. Ramdas, and S. Rodriguez, Phys. Rev. B8, 3836 (1973).
[53]N. V. Alkeev, A. S. Kaminskiĭ, and Ya. Pokrovskiĭ, Fiz. Tverd. Tela (Leningrad) 18, 713 (1976) [Sov. Phys. Solid State 18, 410 (1976)].
[54]P. D. Altukhov, G. E. Pikus, and A. A. Rogachev, Fiz. Tverd. Tela (Leningrad) 20, 489 (1978) [Sov. Phys. Solid State 20, 283 (1978)].
[55]A. S. Kaminskiĭ and Ya. E. Pokrovskiĭ, Zh. Eksp. Teor. Fiz. 76, 1727 (1979) [Sov. Phys. JETP 49, 878 (1979)].
[56]V. D. Kulakovskiĭ, A. V. Malyavkin, and V. B. Timofeev, Pis'ma Zh. Eksp. Teor. Fiz. 27, 576 (1978) [JETP Lett. 27, 542 (1978)]; 28, 58 (1978) [*sic*].
[57]V. D. Kulakovskiĭ, A. V. Malyavkin, and V. B. Timofeev, Zh. Eksp. Teor. Fiz. 76, 272 (1978) [Sov. Phys. JETP 49, 139 (1978)].
[58]W. Schmid, Phys. Status Solidi, B84, 529 (1977).
[59]G. L. Bir and G. E. Picus, in: Proc. of Seventh Intern. Conference on Physics of Semiconductors, Dunod, Paris, Academic Press, 1964.
[60]P. D. Altukhov, K. N. El'tsov, G. E. Pikus, and A. A. Rogachev, Fiz. Tverd. Tela (Leningrad) 22, 239 (1980) [Sov. Phys. Solid State 22, 140 (1980)].
[61]P. D. Altukhov, K. N. El'tsov, G. E. Pikus, and A. A. Rogachev, Pis'ma Zh. Eksp. Teor. Fiz. 26, 468 (1977) [JETP Lett. 26, 337 (1977)].
[62]N. S. Averkiev, P. D. Altukhov, K. N. El'tsov, G. E. Pikus, A. A. Rogachev, and E. M. Ushakova, Fiz. Tverd. Tela (Leningrad) 22, 1980 (1980) [Sov. Phys. Solid State 22, 1154 (1980)].
[63]P. D. Altukhov, K. N. El'tsov, G. E. Pikus, and A. A. Rogachev, Fiz. Tverd. Tela (Leningrad) 22, 599 (1980) [Sov. Phys. Solid State 22, 350 (1980)].
[64]N. S. Averkiev, Fiz. Tverd. Tela (Leningrad) 22, 2493 (1980) [Sov. Phys. Solid State 22, 1454 (1980)].
[65]N. S. Averkiev, P. D. Altukhov, V. M. Asnin, K. N. El'tsov, Yu. N. Lomasov, G. E. Pikus, A. A. Rogachev, and N. A. Rud', in: Materialy II respublikanskogo kollokviuma po modulyatsionnoĭ spektroskopii poluprovodnikov. Sukhumi, 1979 (Proceedings of the Second Georgian Colloquium on Modulation Spectroscopy of Semiconductors, Sukhumi, 1979), Tbilisi, 1980, p. 183.
[66]A. S. Kaminskiĭ, V. A. Karasyuk, and Ya. E. Pokrovskiĭ, Zh. Eksp. Teor. Fiz. 79, 422 (1980) [Sov. Phys. JETP 52, 211 (1980)].
[67]D. K. Wilson and G. Feher, Phys. Rev. 124, 1068 (1961).
[68]F. Merlet, B. Pajot, Ph. Arcas, and A. M. Jean-Louis, Phys. Rev. B12, 3297 (1975).
[69]L. D. Landau and E. M. Lifshitz, Kvantovaya mekhanika, Nauka, Moscow, 1974 (Quantum Mechanics: Non-Relativistic Theory, Pergamon, New York, 1977).
[70]H. -J. Wünsche, K. Henneberger, and V. E. Khartsiev, Phys. Status Solidi, B86, 505 (1978).
[71]A. S. Kaminskiĭ, V. A. Karasyuk, and Ya. E. Pokrovskiĭ, Pis'ma Zh. Eksp. Teor. Fiz. 33, 141 (1981) [JETP Lett. 33, 132 (1981)].
[72]G. E. Pikus and I. S. Averkiev, Pis'ma Zh. Eksp. Teor. Fiz. 34, 28 (1981) [JETP Lett. 34, 26 (1981)].
[73]P. D. Altukhov, K. N. El't sov, G. E. Pikus, and A. A. Rogachev, in: Proc. Fourteenth Intern. Conference on Physics of Semiconductors, Edinburgh, 1978, p. 379.

Translated by Dave Parsons